Applied Thermal Engineering 236 (2024) 121626

Contents lists available at ScienceDirect

Applied Thermal Engineering

journal homepage: www.elsevier.com/locate/ate

Research Paper

Thermal interaction of slender geothermal boreholes with creeping groundwater flows

Javier Rico *, Miguel Hermanns

Departamento de Mecánica de Fluidos y Propulsión Aeroespacial, Escuela Técnica Superior de Ingeniería Aeronáutica y del Espacio, Universidad Politécnica de Madrid, Plaza Cardenal Cisneros 3, E-28040 Madrid, Spain

ARTICLE INFO

Keywords:
Geothermal heat exchangers
Geothermal boreholes
Groundwater flows
Thermal response
Asymptotic expansion
Low peclet number

ABSTRACT

In the presence of groundwater flows, more compact and affordable geothermal heat exchangers can be constructed thanks to the increased heat transfer capabilities of the ground. To correctly design them, theoretical models for the thermal interaction of geothermal boreholes with aquifers are required. By using matched asymptotic expansion techniques, a new theoretical model for the case of creeping groundwater flows is developed in the present work. This new model improves by an order of magnitude the accuracy of the state of the art, leading to absolute (relative) errors below 0.03 (2.3%). Additionally, the mathematically-rigorous and physically-sound derivation of the proposed model allows, for the first time, the assessment of the theoretical and conceptual merits and limits of the state of the art.

1. Introduction

Energy plays a fundamental role in almost every challenge mankind faces nowadays, with the fight against climate change considered the greatest one. Since heating and cooling of buildings is one of the main contributors to world energy consumption, with a share of almost 23% [1], the development of energy-efficient heating, ventilation, and air conditioning (HVAC) systems is considered a key action against climate change.

One of the most attractive solutions is the harnessing of low enthalpy geothermal energy. A geothermal HVAC system consists in a water-to-water heat pump connected to a geothermal heat exchanger comprised of vertical boreholes. As shown in Fig. 1, each of these boreholes is equipped with one or more coaxial or U-shaped probes through which a heat carrying liquid flows to exchange heat with the ground.

The correct sizing of a geothermal heat exchanger is crucial for the successful harnessing of geothermal energy. A size too large leads to high initial investment costs and unreasonable payback times. A size too small implies that, in order to satisfy the heating and cooling needs of the building, more extreme temperatures in the heat carrying liquid are required. This unavoidably leads to a drop in the overall efficiency of the HVAC system.

It is therefore crucial to accurately forecast the thermal response of a geothermal heat exchanger over the whole lifespan of a building, of typically 100 years, in order to correctly design the installation. Detailed numerical simulations of the whole problem, however, are unfeasible for engineering purposes [2–11]. Hence, simplified theoretical models are used instead which are accurate, flexible, and fast.

All theoretical models take into account the conduction of heat in the ground [12,13]. For unfractured igneous and metamorphic rocks and for clayey soils it is the dominant heat transfer mechanism so that the accuracy of predictions in such grounds is high. However, the convective transport of heat due to groundwater flows is often equally relevant, especially in fractured igneous and metamorphic rocks and in gravelly soils [2,3,14–16]. For those grounds, only models that incorporate this second heat transfer mechanism are able to correctly forecast the thermal response of the geothermal heat exchanger.

Theoretical models that account for groundwater flows already exist [17,18]. They are mostly based on the moving point-source of heat theory extensively studied by Carslaw and Jaeger [19]. From it, several models have been derived like the moving infinite line source [14,20–25], the moving finite line source [24–36], the moving infinite cylindrical heat source [4,37–40], or combinations of these three [41–44]. These models work reasonably well but exploit assumptions and simplifications that lack proper mathematical justification or are inconsistent with the physics of the problem. This affects the confidence in their use for real-world engineering tasks. Therefore, the mathematically rigorous derivation of a physically-sound theoretical model would help to judge and clarify these issues and explain why, after all, the existing models work well.

The aim of the present work is precisely the derivation of such a theoretical model. Three objectives are sought thereby. First and

* Corresponding author.
E-mail addresses: j.rico@upm.es (J. Rico), miguel.hermanns@upm.es (M. Hermanns).

https://doi.org/10.1016/j.applthermaleng.2023.121626
Received 23 March 2023; Received in revised form 8 September 2023; Accepted 15 September 2023
Available online 21 September 2023

Nomenclature

$\tilde{A}_{0n}, \tilde{A}_{1n}$	Integration constants of the zeroth order solution and first order correction to the inner region, respectively [–]
$A_{0(\pm1)}$	Integration constants of the zeroth order solution to the inner region in the time domain [–]
A_{0nj}	Weight of $\tilde{\mathrm{q}}_j/(2\pi\kappa)$ in $\tilde{A}_{0n}$ [–]
α_b, α_g	Thermal diffusivity of grout and ground, respectively [m^2/s]
$\tilde{B}_{0n}, \tilde{B}_{1n}$	Integration constants of the zeroth order solution and first order correction to the inner region, respectively [–]
$\tilde{C}_{0n}, \tilde{C}_{1n}$	Integration constants of the zeroth order solution and first order correction to the outer region, respectively [–]
d_j	Thickness of the wall of pipe j [m]
E_1	Exponential integral [–]
$\mathrm{f}, \tilde{\mathrm{f}}$	Non-dimensional fictitious heat injection rate per unit borehole length [–] and its Laplace-transformed counterpart [–]
γ	Euler's constant [–]
HVAC	Heating, Ventilation, and Air Conditioning
H	Depth of the borehole [m]
h_j	Convective heat transfer coefficient of pipe j [$W/(m^2\,K)$]
$\imath$	Imaginary unit [–]
K	Permeability of the ground [m^2]
K_n	Modified Bessel function of the second kind of order n [–]
$\underline{K}_n$	Mathematical function that tends to K_n for large times [–]
k_b, k_g, k_j	Thermal conductivity of grout, ground, and the wall of pipe j, respectively [W/(m K)]
κ	Ratio between the thermal conductivity of grout and the thermal conductivity of ground [–]
λ	Dummy integration variable [–]
$\mathcal{L}$	Non-dimensional Laplace operator [–]
μ	Dynamic viscosity of groundwater [Pa s]
N_p	Number of pipes in the borehole [–]
ω	Non-dimensional angular frequency [–]
p	Effective driving pressure [Pa]
Pe	Peclet number of the groundwater flow [–]
q	Heat injection rate per unit borehole length [W/m]
$\mathrm{q}, \tilde{\mathrm{q}}, \hat{\mathrm{q}}$	Non-dimensional heat injection rate per unit borehole length [–], its Laplace-transformed counterpart [–], and its harmonic counterpart [–]
q_c	Characteristic value for the heat injection rates per unit pipe or borehole length [W/m]
q_j	Heat injection rate per unit pipe length of pipe j [W/m]
$\mathrm{q}_j, \tilde{\mathrm{q}}_j, \hat{\mathrm{q}}_j$	Non-dimensional heat injection rate per unit pipe length of pipe j [–], its Laplace-transformed counterpart [–], and its harmonic counterpart [–]
r, ρ	Radial coordinate of the polar coordinate system centered at the borehole [m] and its non-dimensional counterpart [–]
r_b	Radius of the borehole [m]
r_j, ρ_j	Radial coordinate of the polar coordinate system centered at pipe j [m] and its non-dimensional counterpart [–]
r_{pj}, ρ_{pj}	Radius of pipe j [m] and its non-dimensional counterpart [–]
R_{pj}, R_{pj}	Inner thermal resistance of pipe j [(m K)/W] and its non-dimensional counterpart [–]
s	Non-dimensional position in the complex-valued Laplace plane [–]
T	Grout/ground temperature [K]
$\tilde{\Theta}_{\mathrm{out}}$	Solution to the outer region [–]
$\tilde{\Theta}^{(0)}_{\mathrm{out}}, \tilde{\Theta}^{(1)}_{\mathrm{out}}$	Zeroth order solution and first order correction to outer region, respectively [–]
t_b	Characteristic transversal diffusion time [s]
t_c	Characteristic residence time of groundwater stream in the vicinity of the borehole [s]
t_H	Characteristic longitudinal diffusion time [s]
t_q	Characteristic time of the heat injection/extraction required by the HVAC system [s]
t_r	Characteristic residence time of the heat carrying liquid in the pipes [s]
θ	Angular coordinate of the polar coordinate system centered at the borehole [rad]
θ_j	Angular coordinate of the polar coordinate system centered at pipe j [rad]
$\Theta, \tilde{\Theta}, \hat{\Theta}$	Non-dimensional grout/ground temperature [–], its Laplace-transformed counterpart [–], and its harmonic counterpart [–]
t, τ	Time [s] and its non-dimensional counterpart [–]
T_∞	Unperturbed ground temperature [K]
T_j	Bulk temperature of the fluid in pipe j [K]
$\Theta_j, \tilde{\Theta}_j, \hat{\Theta}_j$	Non-dimensional bulk temperature of the fluid in pipe j [–], its Laplace-transformed counterpart [–], and its harmonic counterpart [–]
$\hat{\Theta}_b$	Non-dimensional harmonic of the mean azimuthal borehole wall temperature [–]
$\tilde{\Theta}^{(0)}_j, \tilde{\Theta}^{(1)}_j$	Zeroth order solution and first order correction to the bulk fluid temperature in pipe j, respectively [–]
$\tilde{\Theta}_{\mathrm{in}}$	Solution to the inner region [–]
$\tilde{\Theta}^{(0)}_{\mathrm{in}}, \tilde{\Theta}^{(1)}_{\mathrm{in}}$	Zeroth order solution and first order correction to the inner region, respectively [–]
U_∞	Effective seepage velocity of the groundwater flow [m/s]
v_r, v_r	Radial component of the effective velocity of the groundwater flow [m/s] and its non-dimensional counterpart [–]
$v_\theta, \mathrm{v}_\theta$	Azimuthal component of the effective velocity of the groundwater flow [m/s] and its non-dimensional counterpart [–]

V	Bulk velocity of the heat carrying liquid [m/s]
w	Second argument of the function $\underline{K}_n$ [–]
x, y	Cartesian coordinates centered at the borehole [m]
z	First argument of the function $\underline{K}_n$ [–]

foremost, to judge and clarify the aforementioned issues in the state of the art. Second, improve the accuracy over the state of the art by an order of magnitude. And third, develop a model that seamlessly integrates into the coherent theoretical framework being pursued by the second author since 2011 [45,46].

The present work is organized as follows. Section 2 formulates the fluid-mechanical and heat transfer problems that describe the interaction of slender geothermal boreholes with creeping groundwater flows. Section 3 analyses then the asymptotic structure of the formulated problem and obtains its solution using matched asymptotic expansion techniques. Thereafter, Section 4 discusses the merits and limits of the proposed model while Section 5 does the same with the state of the art. Sections 6 and 7 focus then on the integration of the proposed model into more complex models. Finally, some concluding remarks are presented in Section 8.

2. Interaction of boreholes with aquifers

Fig. 1 shows the sketch of a typical geothermal borehole that consists in a vertical borehole of depth H and radius r_b into which several pipes are placed forming one or more coaxial or U-shaped probes. The heat carrying liquid flows with a bulk velocity V along these pipes to exchange heat with the surrounding ground. The space between pipes and ground is usually filled up with grout to promote the aforementioned heat exchange and to avoid the cross-contamination of aquifers.

Three characteristic times can be constructed out of the previous parameters, namely, the characteristic residence time $t_r \sim H/V$ of the heat carrying liquid in the pipes, the characteristic transversal diffusion time $t_b \sim r_b^2/\alpha_g$, where α_g is the effective thermal diffusivity of the ground, and the characteristic longitudinal diffusion time $t_H \sim H^2/\alpha_g$. Computing these characteristic times using real-world values for H, r_b, V, and α_g reveals that t_r is of order minutes, t_b is of order hours, and t_H is of order centuries [47].

The heat injection/extraction imposed by the HVAC system onto the geothermal heat exchanger introduces a fourth characteristic time, namely, t_q. Since the heating and cooling needs of a building vary on an hourly, daily, weekly, monthly, and yearly basis, the characteristic time t_q presents a large spectrum of values that go from minutes up to decades [47]. The present work focuses on the most relevant operating conditions for which t_q is much larger than t_b but much smaller than t_H. This leads to the sequence of characteristic times

$$t_r \ll t_b \ll t_q \ll t_H.$$

This disparity in time scales has extensively been exploited by the second author for the development of theoretical models for the thermal response of geothermal heat exchangers in purely-conducting grounds [47–53].

The aim of the present work is to incorporate the effect of groundwater flows in the thermal response of geothermal boreholes. Hence, a fifth characteristic time emerges, namely, the characteristic residence time $t_c \sim r_b/U_\infty$ of the groundwater stream in the vicinity of the borehole, where U_∞ is the effective seepage velocity of the groundwater flow [20,23,32]. The ratio of t_c to the characteristic transversal diffusion time t_b is of the order of the Peclet number of the groundwater flow:

$$\mathrm{Pe} = \frac{r_b U_\infty}{\alpha_g} \sim \frac{t_b}{t_c}. \tag{1}$$

The Peclet number measures the relative importance of convective terms over diffusive terms in the energy conservation equation in the ground [54]. Hence, in creeping groundwater flows, for which the convective transport of heat is weak, the Peclet number is small compared to unity. This fact will be exploited in the present work to derive approximate, albeit accurate, solutions to the thermal interaction of geothermal boreholes with creeping groundwater flows.

2.1. Fluid-mechanical problem

The thermal response of a geothermal borehole depends on the groundwater's velocity field as it flows around the borehole. Hence, its governing equations, i.e. mass and momentum conservation, need to be solved. To do so, the porous medium approach [55] is used to avoid formulating and solving the governing equations in the small voids of the soil.

Due to the extreme slenderness of real-world geothermal boreholes, $r_b \ll H$, groundwater movement along the borehole is negligible compared to the mainstream flow. Therefore, the groundwater motion can be described through independent two-dimensional fluid-mechanical problems formulated in planes perpendicular to the borehole. Fig. 1 shows one of those planes.

The mass conservation equation for a constant-density flow in a porous medium is, for one of those two-dimensional planes perpendicular to the borehole [55],

$$\frac{\partial}{\partial r}(r v_r) + \frac{\partial v_\theta}{\partial \theta} = 0,$$

where (r, θ) are the coordinates in the polar coordinate system centered at the borehole, with v_r and v_θ being the effective velocity components in the radial and azimuthal directions, respectively.

In the porous medium approach, the momentum conservation equation is always replaced by an empirical law. Since groundwater flows of interest are governed by viscous forces, Darcy's law is employed in the present work [55],

$$v_r = -\frac{K}{\mu}\frac{\partial p}{\partial r} \qquad \text{and} \qquad v_\theta = -\frac{K}{\mu}\frac{1}{r}\frac{\partial p}{\partial \theta},$$

being p the effective driving pressure. The permeability K of the ground and the dynamic viscosity μ of the groundwater are both functions of depth so that the values to use here correspond to the ones at the depth of the considered plane.

Once the governing equations for the groundwater motion have been established, conditions at each boundary of the problem must be formulated. So, a slip condition is imposed at the borehole wall to enforce there an impermeable behavior:

$$r = r_b : \; v_r = 0.$$

And far from the borehole the velocity field must match the unperturbed effective seepage velocity U_∞ of the aquifer at the depth of the considered plane. This uniform stream condition translates into the following boundary conditions for v_r and v_θ:

$$r \to \infty : \; v_r \to U_\infty \cos(\theta), \; v_\theta \to -U_\infty \sin(\theta).$$

For constant values of permeability K and dynamic viscosity μ, the just-formulated fluid-mechanical problem is analogous to the problem of potential flow past a circular cylinder. This fact is relevant as the latter problem can be solved exactly [56] leading to the following expressions for the effective velocity components of the groundwater flow:

$$v_r = U_\infty\left(1 - \frac{r_b^2}{r^2}\right)\cos(\theta),$$

$$v_\theta = -U_\infty\left(1 + \frac{r_b^2}{r^2}\right)\sin(\theta).$$

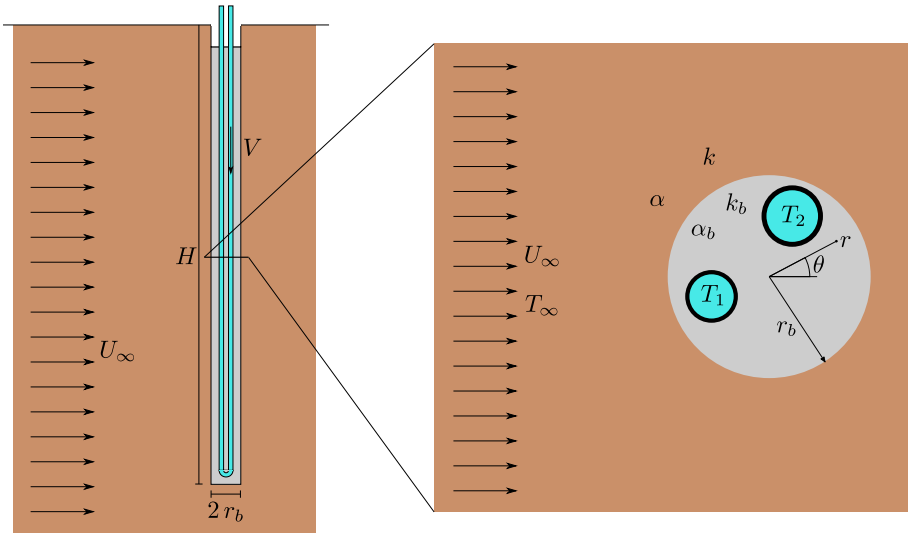

Fig. 1. Sketch of a typical geothermal borehole.

2.2. Thermal problem

Also the heat transfer problem in the ground can be described through independent two-dimensional problems formulated in planes perpendicular to the borehole. The simplification is a consequence of $t_q \ll t_H$ which implies that heat conduction along the borehole is negligible compared to heat conduction in the radial direction [47]. This simplification does not affect the possible dependence with depth of the thermal properties of ground, aquifer, grout, etc., with their values at the depth of the considered plane being the ones to use throughout the present work.

As with the fluid-mechanical problem presented before, the porous medium approach is used to avoid formulating and solving the aforementioned heat transfer problems in the intricate voids of the ground. Additionally, local thermal equilibrium between soil and groundwater is assumed as the motion of the latter is dominated by viscous forces [55]. As a result, a single convection–diffusion energy conservation equation with an effective thermal diffusivity α_g and the effective groundwater velocity (v_r, v_θ) computed before governs the thermal response of the ground [55]:

$$\frac{\partial T}{\partial t} + v_r \frac{\partial T}{\partial r} + \frac{v_\theta}{r}\frac{\partial T}{\partial \theta} = \alpha_g \left[\frac{1}{r}\frac{\partial}{\partial r}\left(r \frac{\partial T}{\partial r} \right) + \frac{1}{r^2}\frac{\partial^2 T}{\partial \theta^2} \right].$$

When writing this equation, constant thermal properties have been assumed for the ground. This simplification is justified by the small temperature variations expected in the problem, at most of 10 °C-20 °C, which lead to negligible variations in the involved thermal characteristics. The same assumption has also been used in the previous section for the permeability K and for the dynamic viscosity μ.

For the heat conduction taking place in the grout filling up the borehole, the previously-described simplifications apply as well so that the two-dimensional unsteady heat conduction equation to solve is

$$\frac{\partial T}{\partial t} = \alpha_b \left[\frac{1}{r}\frac{\partial}{\partial r}\left(r \frac{\partial T}{\partial r} \right) + \frac{1}{r^2}\frac{\partial^2 T}{\partial \theta^2} \right],$$

with α_b being the thermal diffusivity of grout.

The solution to the formulated governing equations must also satisfy the following continuity conditions in temperature and normal heat flux at the borehole wall:

$$T\Big|_{r=r_b^-} = T\Big|_{r=r_b^+} \quad \text{and} \quad -k_b \frac{\partial T}{\partial r}\Big|_{r=r_b^-} = -k_g \frac{\partial T}{\partial r}\Big|_{r=r_b^+},$$

where k_g is the effective thermal conductivity of ground and k_b is the thermal conductivity of grout.

The solution must also obey boundary conditions at the N_p pipes forming the coaxial or U-shaped probes located inside the borehole. These specify the normal heat flux at the outer wall of each pipe j in terms of the bulk temperature $T_j(t)$ of the liquid inside the pipe and the temperature attained by the grout at the pipe wall [47]:

$$-k_b r_{pj} \frac{\partial T}{\partial r_j}\Big|_{r_j=r_{pj}} = \frac{T_j(t) - T\Big|_{r_j=r_{pj}}}{R_{pj}}, \tag{2}$$

where r_{pj} is the outer pipe radius and (r_j, θ_j) are the coordinates of a polar coordinate system centered at pipe j.

All heat transfer taking place inside pipe j is represented in the formulated boundary condition by the inner thermal resistance R_{pj}. It encompasses the quasi-steady heat conduction inside the pipe's wall, of thickness d_j and thermal conductivity k_j, and the turbulent transport of heat inside the heat carrying liquid, modeled through a convective heat transfer coefficient h_j [47]:

$$R_{pj} = \frac{1}{(r_{pj} - d_j)h_j} + \frac{1}{k_j} \ln\left(\frac{r_{pj}}{r_{pj} - d_j} \right).$$

Finally, the solution to the formulated problem must tend to the unperturbed ground temperature T_∞, at the depth of the considered plane, far away from the borehole and at the beginning of the problem:

$$r \to \infty : T \to T_\infty,$$

$$t = 0 : T = T_\infty.$$

Given the fluid temperatures $T_j(t)$, the just-formulated problem delivers the temperature distribution $T(r, \theta, t)$ in grout and ground. However, the known quantities are often not the fluid temperatures but the heat injection rates per unit pipe length $q_j(t)$ [50,53,57–59]:

$$q_j(t) = \int_{-\pi}^{\pi} -k_b \frac{\partial T}{\partial r_j}\Big|_{r_j=r_{pj}} r_{pj}\, \mathrm{d}\theta_j.$$

These and the fluid temperatures T_j in the pipes vary along the borehole [47–49,52] as a result of the convective transport of heat along the pipes and the dependence with depth of the thermal properties and unperturbed state of grout and ground. These variations, however, play a secondary role in the thermal problem to solve here so that only their values at the depth of the considered plane are important.

When q_j are the known quantities, the formulated heat transfer problem delivers not only the temperature distribution in grout and ground but also the fluid temperatures $T_j(t)$ required to enforce the specified heat injection rates per unit pipe length. These result from

solving Eq. (2) for the fluid temperature and averaging then the outcome along the pipe wall:

$$T_j(t) = \frac{R_{pj}}{2\pi} q_j(t) + \frac{1}{2\pi}\int_{-\pi}^{\pi} T\Big|_{r_j=r_{pj}} \mathrm{d}\theta_j.$$

In the present work this same *modus operandi* is adopted for which the heat injection rate per unit borehole length $q(t)$ is defined as well as it appears in the solution to obtain:

$$q(t) = \sum_{j=1}^{N_p} q_j(t).$$

2.2.1. Non-dimensionalization

The formulated problem is non-dimensionalized to facilitate its analysis and solution. For that purpose, the radius of the borehole r_b and the characteristic transversal diffusion time r_b^2/α_g are chosen as characteristic length and time scales so that $\rho = r/r_b$ and $\tau = \alpha_g t/r_b^2$ are the resulting non-dimensional radial and time variables, respectively.

On the other hand, the effective seepage velocity U_∞ is employed for the non-dimensional velocity components:

$$\begin{aligned} \mathrm{v}_\rho &= \left(1 - \frac{1}{\rho^2}\right)\cos(\theta), \\ \mathrm{v}_\theta &= -\left(1 + \frac{1}{\rho^2}\right)\sin(\theta). \end{aligned} \tag{3}$$

Similarly, all heat injection rates per unit pipe length are non-dimensionalized using a characteristic value q_c, i.e. the maximum or the mean, and all temperatures are non-dimensionalized using q_c/k_g as characteristic temperature difference. Hence,

$$\mathrm{q}_j = \frac{q_j}{q_c}, \qquad \Theta = \frac{T - T_\infty}{q_c/k_g}, \qquad \text{and} \qquad \Theta_j = \frac{T_j - T_\infty}{q_c/k_g}.$$

With the proposed non-dimensionalization, the energy conservation equation in the ground becomes

$$\frac{\partial\Theta}{\partial\tau} + \mathrm{Pe}\left[\mathrm{v}_\rho\frac{\partial\Theta}{\partial\rho} + \frac{\mathrm{v}_\theta}{\rho}\frac{\partial\Theta}{\partial\theta}\right] = \frac{1}{\rho}\frac{\partial}{\partial\rho}\left(\rho\frac{\partial\Theta}{\partial\rho}\right) + \frac{1}{\rho^2}\frac{\partial^2\Theta}{\partial\theta^2},$$

while the energy conservation equation in the grout is now

$$\frac{\alpha_g}{\alpha_b}\frac{\partial\Theta}{\partial\tau} = \frac{1}{\rho}\frac{\partial}{\partial\rho}\left(\rho\frac{\partial\Theta}{\partial\rho}\right) + \frac{1}{\rho^2}\frac{\partial^2\Theta}{\partial\theta^2}.$$

Regarding the continuity conditions in temperature and normal heat flux at the borehole wall, they adopt the following non-dimensional form in which $\kappa = k_b/k_g$:

$$\Theta\Big|_{\rho=1^-} = \Theta\Big|_{\rho=1^+}, \qquad -\kappa\frac{\partial\Theta}{\partial\rho}\Big|_{\rho=1^-} = -\frac{\partial\Theta}{\partial\rho}\Big|_{\rho=1^+}. \tag{4}$$

In the boundary conditions to enforce at the wall of each pipe j, the non-dimensional inner thermal resistance of the pipe $\mathrm{R}_{pj} = k_g R_{pj}$ emerges as a parameter to take into account,

$$-\rho_{pj}\kappa\frac{\partial\Theta}{\partial\rho_j}\Big|_{\rho_j=\rho_{pj}} = \frac{\Theta_j - \Theta\big|_{\rho_j=\rho_{pj}}}{\mathrm{R}_{pj}}, \tag{5}$$

where $\rho_j = r_j/r_b$ and $\rho_{pj} = r_{pj}/r_b$. The same happens in the expression that delivers the fluid temperatures in the pipes:

$$\Theta_j(\tau) = \frac{\mathrm{R}_{pj}}{2\pi}\mathrm{q}_j(\tau) + \frac{1}{2\pi}\int_{-\pi}^{\pi}\Theta\Big|_{\rho_j=\rho_{pj}}\mathrm{d}\theta_j. \tag{6}$$

And the boundary condition far from the borehole as well as the initial condition for the problem become homogeneous thanks to the employed non-dimensionalization for the temperatures:

$$\begin{aligned} &\rho \to \infty : \Theta \to 0, \\ &\tau = 0 : \Theta = 0. \end{aligned} \tag{7}$$

Finally, heat injection rates per unit pipe length and per unit borehole length non-dimensionalize as follows:

$$\mathrm{q}_j(\tau) = \int_{-\pi}^{\pi} -\kappa\frac{\partial\Theta}{\partial\rho_j}\Big|_{\rho_j=\rho_{pj}}\rho_{pj}\,\mathrm{d}\theta_j,$$

$$\mathrm{q}(\tau) = \sum_{j=1}^{N_p}\mathrm{q}_j(\tau).$$

2.2.2. Laplace transformation

Time dependence of the formulated heat transfer problem is addressed using the Laplace transform [60]. Most of the problem formulated and non-dimensionalized in previous sections remains thereby unaltered, with just temperatures and heat injection rates per unit pipe or borehole length bearing now a tilde (∼) to denote their Laplace-transformed character.

Only the two energy conservation equations change with the application of the Laplace transform. So, the energy conservation equation in the ground gets transformed into the following expression in which s stands for the non-dimensional position in the complex-valued Laplace plane:

$$s\,\tilde{\Theta} + \mathrm{Pe}\left[\mathrm{v}_\rho\frac{\partial\tilde{\Theta}}{\partial\rho} + \frac{\mathrm{v}_\theta}{\rho}\frac{\partial\tilde{\Theta}}{\partial\theta}\right] = \frac{1}{\rho}\frac{\partial}{\partial\rho}\left(\rho\frac{\partial\tilde{\Theta}}{\partial\rho}\right) + \frac{1}{\rho^2}\frac{\partial^2\tilde{\Theta}}{\partial\theta^2}. \tag{8}$$

And the energy conservation equation in the grout becomes

$$s\frac{\alpha_g}{\alpha_b}\tilde{\Theta} = \frac{1}{\rho}\frac{\partial}{\partial\rho}\left(\rho\frac{\partial\tilde{\Theta}}{\partial\rho}\right) + \frac{1}{\rho^2}\frac{\partial^2\tilde{\Theta}}{\partial\theta^2}. \tag{9}$$

3. Asymptotic solution to thermal problem

The heat transfer problem to solve, summarized in Table 1, is comprised of two governing equations, Eqs. (8) and (9), continuity conditions at the borehole wall, Eq. (4), boundary conditions at the pipe walls, Eqs. (5) and (6), and a boundary condition far from the borehole, Eq. (7).

In the absence of an exact solution, the present work derives an approximate, albeit accurate, one using matched asymptotic expansion techniques [61]. These techniques exploit the presence of small parameters to decompose mathematically complex problems into simpler ones. Hence, they are perfectly suited for the present problem in which a small parameter exists, namely, the Peclet number of the groundwater flow.

Consider the energy conservation equation in the ground, Eq. (8), and estimate the order of magnitude of the three groups of terms present in it [54]:

$$\underbrace{s\,\tilde{\Theta}}_{\sim|s|} + \underbrace{\mathrm{Pe}\left[\mathrm{v}_\rho\frac{\partial\tilde{\Theta}}{\partial\rho} + \frac{\mathrm{v}_\theta}{\rho}\frac{\partial\tilde{\Theta}}{\partial\theta}\right]}_{\sim\mathrm{Pe}/\rho} = \underbrace{\frac{1}{\rho}\frac{\partial}{\partial\rho}\left(\rho\frac{\partial\tilde{\Theta}}{\partial\rho}\right) + \frac{1}{\rho^2}\frac{\partial^2\tilde{\Theta}}{\partial\theta^2}}_{\sim 1/\rho^2}.$$

3.1. Two-region structure

Three factors influence the relative importance of these groups. First, the modulus of the position s in the complex-valued Laplace plane dictates the order of magnitude of the leftmost group, linked to the thermal inertia of the ground. As explained in Rivero and Hermanns [53], $|s| \sim t_b/t_q$ so that in the present work $|s| \ll 1$. Second, the Peclet number of the flow influences the order of magnitude of the central group of terms, linked to the convective transport of heat in the ground. Since the present work focuses on creeping groundwater flows, $\mathrm{Pe} \ll 1$. And third, the distance ρ to the borehole affects the order of magnitude of the second and third groups of terms, with the third one representing heat conduction in the ground. All this allows the identification of two distinct regions in the problem.

Close to the borehole, at radial distances comparable to the borehole radius, $\rho \sim 1$. There, thermal inertia and convective transport of heat are negligible compared to heat conduction as a consequence of

Table 1
Formulation of the heat transfer problem to solve.

Energy conservation in ground:

$$s\,\tilde{\Theta} + \mathrm{Pe}\left[\mathrm{v}_\rho \frac{\partial\tilde{\Theta}}{\partial\rho} + \frac{\mathrm{v}_\theta}{\rho}\frac{\partial\tilde{\Theta}}{\partial\theta}\right] = \frac{1}{\rho}\frac{\partial}{\partial\rho}\left(\rho\frac{\partial\tilde{\Theta}}{\partial\rho}\right) + \frac{1}{\rho^2}\frac{\partial^2\tilde{\Theta}}{\partial\theta^2}$$

with

$$\mathrm{v}_\rho = \left(1 - \frac{1}{\rho^2}\right)\cos(\theta) \qquad \text{and} \qquad \mathrm{v}_\theta = -\left(1 + \frac{1}{\rho^2}\right)\sin(\theta)$$

Energy conservation in grout:

$$s\,\frac{\alpha_g}{\alpha_b}\tilde{\Theta} = \frac{1}{\rho}\frac{\partial}{\partial\rho}\left(\rho\frac{\partial\tilde{\Theta}}{\partial\rho}\right) + \frac{1}{\rho^2}\frac{\partial^2\tilde{\Theta}}{\partial\theta^2}$$

Continuity conditions at borehole wall:

$$\tilde{\Theta}\Big|_{\rho=1^-} = \tilde{\Theta}\Big|_{\rho=1^+} \qquad \text{and} \qquad -\kappa\frac{\partial\tilde{\Theta}}{\partial\rho}\Big|_{\rho=1^-} = -\frac{\partial\tilde{\Theta}}{\partial\rho}\Big|_{\rho=1^+}$$

Boundary condition far from the borehole:

$$\rho \to \infty : \ \tilde{\Theta} \to 0$$

Boundary condition at the wall of pipe j

$$-\rho_{pj}\kappa\frac{\partial\tilde{\Theta}}{\partial\rho_j}\Big|_{\rho_j=\rho_{pj}} = \frac{\tilde{\Theta}_j - \tilde{\Theta}\big|_{\rho_j=\rho_{pj}}}{\mathrm{R}_{pj}}$$

with

$$\tilde{\Theta}_j = \frac{\mathrm{R}_{pj}}{2\pi}\tilde{\mathrm{q}}_j + \frac{1}{2\pi}\int_{-\pi}^{\pi}\tilde{\Theta}\Big|_{\rho_j=\rho_{pj}}\mathrm{d}\theta_j$$

$|s| \ll 1$ and $\mathrm{Pe} \ll 1$, respectively. Hence, this *inner region* is, in first approximation, quasi-steady and solely governed by heat conduction.

Further away from the borehole, however, the described balance of terms changes giving rise to a second region. So, at distances from the borehole of order $\rho \sim 1/\sqrt{|s|} \gg 1$, thermal inertia and heat conduction become equally important in the governing equation. The relevance of the convective transport of heat in this *outer region* depends then on how $\mathrm{Pe}/\rho \sim \mathrm{Pe}\sqrt{|s|}$ compares to the order of magnitude of the dominant terms. That is, to $|s|$.

The present work focuses on the richest and most general case possible for which all three phenomena (thermal inertia, heat convection, and heat conduction) are important in the outer region. This occurs for the distinguished limit of $\mathrm{Pe}\sqrt{|s|} \sim |s|$. This condition combined with Eq. (1) and with the fact that $|s| \sim t_b/t_q$ allows to properly incorporate the characteristic residence time t_c of the groundwater flow into the sequence of characteristic times of Section 2:

$$t_r \ll t_b \ll t_c \sim \mathrm{Pe}\,t_q \ll t_q \ll t_H .$$

3.2. Matched asymptotic expansion techniques

The two-region structure described before is exploited next using matched asymptotic expansion techniques [61]. These mathematical tools address the inner and outer regions separately to afterwards match their solutions at an overlapping zone in which both solutions are valid. To tackle each of the two regions, asymptotic expansion techniques exploit the presence of small parameters in the problem and express the solutions to the inner and outer regions, $\tilde{\Theta}_{\mathrm{in}}$ and $\tilde{\Theta}_{\mathrm{out}}$ respectively, as polynomial expansions of that small parameter. In the present work, $\mathrm{Pe} \sim \sqrt{|s|} \ll 1$ acts as the small parameter and the expansions to use are

$$\begin{aligned}\tilde{\Theta}_{\mathrm{in}} &= \tilde{\Theta}_{\mathrm{in}}^{(0)} + \mathrm{Pe}\,\tilde{\Theta}_{\mathrm{in}}^{(1)} + \mathcal{O}\left(\mathrm{Pe}^2\right),\\ \tilde{\Theta}_{\mathrm{out}} &= \tilde{\Theta}_{\mathrm{out}}^{(0)} + \mathrm{Pe}\,\tilde{\Theta}_{\mathrm{out}}^{(1)} + \mathcal{O}\left(\mathrm{Pe}^2\right).\end{aligned} \tag{10}$$

Although logarithmic dependencies on the small parameter, of the form $\ln(\mathrm{Pe})$, do appear as well in the asymptotic solution of the problem, these are treated as simple numbers instead and are incorporated as such into the zeroth order solution and first order correction to obtain.

Since the formulated heat transfer problem also supplies the fluid temperatures in the pipes, $\tilde{\Theta}_j$, these must be expanded as well in terms of the small parameter so that

$$\tilde{\Theta}_j = \tilde{\Theta}_j^{(0)} + \mathrm{Pe}\,\tilde{\Theta}_j^{(1)} + \mathcal{O}\left(\mathrm{Pe}^2\right). \tag{11}$$

Substitution of all these expansions into the governing equations, continuity conditions, and boundary conditions of the inner and outer regions supplies a set of mathematical problems whose sequential solution delivers the different terms of the expansions.

3.3. Zeroth order solution

The zeroth order solution to the problem comprises $\tilde{\Theta}_{\mathrm{in}}^{(0)}$, $\tilde{\Theta}_{\mathrm{out}}^{(0)}$, and $\tilde{\Theta}_j^{(0)}$. The corresponding mathematical problems result from substituting Eqs. (10) and (11) into the heat transfer problem formulated in Section 2 and neglecting all terms that are small compared to unity. When doing so, special attention must be devoted to the order of magnitude of ρ as it changes from the inner to the outer region.

3.3.1. Inner region

The borehole itself and the ground located at non-dimensional distances of order unity, $\rho \sim 1$, define the inner region. Since $|s| \ll 1$ and $\mathrm{Pe} \ll 1$, the left hand sides of Eqs. (8) and (9) are negligible so that the zeroth order solution to the inner region satisfies the following equation in grout and ground:

$$0 = \frac{1}{\rho}\frac{\partial}{\partial\rho}\left(\rho\frac{\partial\tilde{\Theta}_{\mathrm{in}}^{(0)}}{\partial\rho}\right) + \frac{1}{\rho^2}\frac{\partial^2\tilde{\Theta}_{\mathrm{in}}^{(0)}}{\partial\theta^2}. \tag{12}$$

This equation must be solved together with the continuity conditions at the borehole wall,

$$\tilde{\Theta}_{\mathrm{in}}^{(0)}\Big|_{\rho=1^-} = \tilde{\Theta}_{\mathrm{in}}^{(0)}\Big|_{\rho=1^+}, \qquad -\kappa\frac{\partial\tilde{\Theta}_{\mathrm{in}}^{(0)}}{\partial\rho}\Big|_{\rho=1^-} = -\frac{\partial\tilde{\Theta}_{\mathrm{in}}^{(0)}}{\partial\rho}\Big|_{\rho=1^+}, \tag{13}$$

the boundary conditions at the pipe walls,

$$-\rho_{pj}\kappa\frac{\partial\tilde{\Theta}_{\mathrm{in}}^{(0)}}{\partial\rho_j}\Big|_{\rho_j=\rho_{pj}} = \frac{\tilde{\Theta}_j^{(0)} - \tilde{\Theta}_{\mathrm{in}}^{(0)}\big|_{\rho_j=\rho_{pj}}}{\mathrm{R}_{pj}}, \tag{14}$$

and the prescribed heat injection rates per unit pipe length:

$$\tilde{\mathrm{q}}_j = \int_{-\pi}^{\pi} -\kappa\frac{\partial\tilde{\Theta}_{\mathrm{in}}^{(0)}}{\partial\rho_j}\Big|_{\rho_j=\rho_{pj}}\rho_{pj}\,\mathrm{d}\theta_j .$$

What cannot be enforced in the inner region is the boundary condition at infinity due to the existence of the outer region. Consequently, Eq. (7) is replaced by an asymptotic matching condition with the zeroth order solution to the outer region.

An exact solution to the formulated problem is unknown. Fortunately, it is not required for the theoretical work to perform as it is enough to know the general behavior of the zeroth order solution in the ground. This behavior is inferred from the general solution to the partial differential equation valid in the ground. That is, Eq. (12):

$$\tilde{\Theta}_{\mathrm{in}}^{(0)}\Big|_{\rho\geq 1} = \tilde{A}_{00} + \tilde{B}_{00}\ln(\rho) + \sum_{\substack{n=-\infty\\ n\neq 0}}^{\infty}\left(\frac{\tilde{A}_{0n}}{\rho^{|n|}} + \rho^{|n|}\tilde{B}_{0n}\right)\mathrm{e}^{\imath n\theta}. \tag{15}$$

In this expression $\imath = \sqrt{-1}$ and the values of the integration constants $\tilde{A}_{0n}$ and $\tilde{B}_{0n}$ result either from the continuity conditions at the borehole wall, assuming the solution in the grout is known, or from the asymptotic matching with the zeroth order solution to the outer region.

For the time being, only $\tilde{B}_{00}$ is obtained. In the absence of thermal inertia, the heat injection rate per unit borehole length $\tilde{\mathrm{q}}$ coincides with the heat flux at the borehole wall integrated over the whole borehole wall. The value of $\tilde{B}_{00}$ results from the enforcement of this equality:

$$\tilde{\mathrm{q}} = \int_{-\pi}^{\pi} -\frac{\partial\tilde{\Theta}_{\mathrm{in}}^{(0)}}{\partial\rho}\Big|_{\rho=1}\mathrm{d}\theta \qquad \rightarrow \qquad \tilde{B}_{00} = -\frac{\tilde{\mathrm{q}}}{2\pi}.$$

Finally, substitution of Eqs. (10) and (11) into Eq. (6) delivers the zeroth order approximation to the fluid temperatures in the pipes:

$$\tilde{\Theta}_j^{(0)} = \frac{R_{pj}}{2\pi}\,\tilde{q}_j + \frac{1}{2\pi}\int_{-\pi}^{\pi} \tilde{\Theta}_{in}^{(0)}\Big|_{\rho_j=\rho_{pj}}\,d\theta_j. \tag{16}$$

3.3.2. Outer region

Far from the borehole, at non-dimensional distances of order $\rho \sim 1/\sqrt{|s|} \sim 1/\mathrm{Pe} \gg 1$, all terms in Eq. (8) are important. Nonetheless, the governing equation becomes solvable in the outer region thanks to the simplifications experienced by the velocity field, Eq. (3), far from the borehole:

$$\begin{aligned} v_\rho\Big|_{\rho\sim 1/\mathrm{Pe}} &= \cos(\theta) + \mathcal{O}(\mathrm{Pe}^2),\\ v_\theta\Big|_{\rho\sim 1/\mathrm{Pe}} &= -\sin(\theta) + \mathcal{O}(\mathrm{Pe}^2). \end{aligned} \tag{17}$$

Hence, the zeroth order solution to the outer region must satisfy the boundary condition far from the borehole, Eq. (7), and the partial differential equation

$$s\,\tilde{\Theta}_{out}^{(0)} + \mathrm{Pe}\left[\cos(\theta)\frac{\partial\tilde{\Theta}_{out}^{(0)}}{\partial\rho} - \frac{\sin(\theta)}{\rho}\frac{\partial\tilde{\Theta}_{out}^{(0)}}{\partial\theta}\right] = \frac{1}{\rho}\frac{\partial}{\partial\rho}\left(\rho\frac{\partial\tilde{\Theta}_{out}^{(0)}}{\partial\rho}\right) + \frac{1}{\rho^2}\frac{\partial^2\tilde{\Theta}_{out}^{(0)}}{\partial\theta^2}.$$

The solution to the formulated problem is

$$\tilde{\Theta}_{out}^{(0)} = e^{\frac{\rho\mathrm{Pe}}{2}\cos(\theta)}\sum_{n=-\infty}^{\infty}\tilde{C}_{0n}\,K_n\left(\frac{\rho\mathrm{Pe}}{2}\sqrt{1+\frac{4s}{\mathrm{Pe}^2}}\right)e^{in\theta}, \tag{18}$$

where $K_n(z)$ stands for the modified Bessel function of the second kind of order n [62]. The yet-unspecified integration constants $\tilde{C}_{0n}$ result from the asymptotic matching of this expression with the zeroth order solution to the inner region. This matching replaces all boundary and continuity conditions specified at the borehole as these cannot be enforced onto the outer region due to the existence of the inner region.

3.3.3. Matching of both regions

At an intermediate distance, located beyond the inner region ($\rho \gg 1$) but closer to the borehole than the outer region ($\rho \ll 1/\mathrm{Pe}$, or alternatively $\rho\mathrm{Pe} \ll 1$), both inner and outer solutions must be equivalent. Hence, their difference must be negligible in this overlapping region, a condition that is expressed mathematically as

$$\tilde{\Theta}_{in}^{(0)}\Big|_{\rho\gg 1} - \tilde{\Theta}_{out}^{(0)}\Big|_{\rho\mathrm{Pe}\ll 1} \ll 1.$$

To enforce it, the behavior of the inner solution far from the borehole, given directly by Eq. (15), has to be compared against Eq. (18) expanded for small values of ρPe:

$$\begin{aligned} \tilde{\Theta}_{out}^{(0)}\Big|_{\rho\mathrm{Pe}\ll 1} &= \tilde{C}_{00}\left[-\ln\left(\frac{\rho\mathrm{Pe}}{4}\sqrt{1+\frac{4s}{\mathrm{Pe}^2}}\right) - \gamma + \mathcal{O}(\mathrm{Pe})\right]\\ &\quad + \sum_{\substack{n=-\infty\\ n\neq 0}}^{\infty}\tilde{C}_{0n}\left[\frac{2^{|n|-1}\,(|n|-1)!}{\left(\frac{\rho\mathrm{Pe}}{2}\sqrt{1+\frac{4s}{\mathrm{Pe}^2}}\right)^{|n|}} + \mathcal{O}\left(\mathrm{Pe}^{1-|n|}\right)\right]e^{in\theta}. \end{aligned}$$

The comparison reveals that the integration constants $\tilde{C}_{00}$ and $\tilde{A}_{00}$ must be as follows in order for the first two terms in Eq. (15) match the corresponding terms in the zeroth order outer solution:

$$\tilde{C}_{00} = -\tilde{B}_{00} = \frac{\tilde{q}}{2\pi},$$

$$\tilde{A}_{00} = \frac{\tilde{q}}{2\pi}\left[-\ln\left(\frac{\mathrm{Pe}}{4}\sqrt{1+\frac{4s}{\mathrm{Pe}^2}}\right) - \gamma\right].$$

The comparison also reveals that all $\tilde{B}_{0n}$ must be zero as no positive powers of ρ exist among the leading terms of the expansion close to the borehole of the zeroth order outer solution. Finally, also the values of $\tilde{C}_{0n}$ with $n \neq 0$ must be zero despite the existence of terms with negative powers of ρ in the zeroth order inner solution. The reason is that the matching of both expressions requires the integration constants $\tilde{C}_{0n}$ to be of order $\mathrm{Pe}^{|n|}$. Hence, they do not belong to the zeroth order level of the asymptotic expansion of the problem but to higher order corrections.

In summary, the asymptotic matching of the zeroth order inner and outer solutions leads to the following final expressions for the zeroth order inner and outer solutions:

$$\tilde{\Theta}_{in}^{(0)}\Big|_{\rho\geq 1} = \tilde{A}_{00} - \frac{\tilde{q}}{2\pi}\ln(\rho) + \sum_{\substack{n=-\infty\\ n\neq 0}}^{\infty}\frac{\tilde{A}_{0n}}{\rho^{|n|}}e^{in\theta}, \tag{19}$$

$$\tilde{\Theta}_{out}^{(0)} = \frac{\tilde{q}}{2\pi}\,e^{\frac{\rho\mathrm{Pe}}{2}\cos(\theta)}K_0\left(\frac{\rho\mathrm{Pe}}{2}\sqrt{1+\frac{4s}{\mathrm{Pe}^2}}\right), \tag{20}$$

where for the sake of compactness the expression for $\tilde{A}_{00}$ has not been substituted.

3.4. First order correction

The first order correction to the problem consists in $\tilde{\Theta}_{in}^{(1)}$, $\tilde{\Theta}_{out}^{(1)}$, and $\tilde{\Theta}_j^{(1)}$. As before, the corresponding mathematical problems result from substituting Eqs. (10) and (11) into the heat transfer problem formulated in Section 2. Now, the terms of order Pe are retained so that the next level of the asymptotic expansion of the problem is analyzed. Thus, only the terms smaller than Pe are discarded.

3.4.1. Inner region

In the inner region, where $\rho \sim 1$, the partial differential equation to solve in the ground includes now an additional term involving the zeroth order solution obtained before:

$$v_\rho\frac{\partial\tilde{\Theta}_{in}^{(0)}}{\partial\rho} + \frac{v_\theta}{\rho}\frac{\partial\tilde{\Theta}_{in}^{(0)}}{\partial\theta} = \frac{1}{\rho}\frac{\partial}{\partial\rho}\left(\rho\frac{\partial\tilde{\Theta}_{in}^{(1)}}{\partial\rho}\right) + \frac{1}{\rho^2}\frac{\partial^2\tilde{\Theta}_{in}^{(1)}}{\partial\theta^2}. \tag{21}$$

In the grout, however, the equation to solve is the same as before as no convective heat transfer exists and thermal inertia is still negligible at this level of the asymptotic expansion of the problem:

$$0 = \frac{1}{\rho}\frac{\partial}{\partial\rho}\left(\rho\frac{\partial\tilde{\Theta}_{in}^{(1)}}{\partial\rho}\right) + \frac{1}{\rho^2}\frac{\partial^2\tilde{\Theta}_{in}^{(1)}}{\partial\theta^2}. \tag{22}$$

The two differential equations must be solved together with the continuity conditions at the borehole wall

$$\tilde{\Theta}_{in}^{(1)}\Big|_{\rho=1^-} = \tilde{\Theta}_{in}^{(1)}\Big|_{\rho=1^+}, \qquad -\kappa\frac{\partial\tilde{\Theta}_{in}^{(1)}}{\partial\rho}\Big|_{\rho=1^-} = -\frac{\partial\tilde{\Theta}_{in}^{(1)}}{\partial\rho}\Big|_{\rho=1^+} \tag{23}$$

and the boundary conditions at the pipe walls

$$-\rho_{pj}\kappa\frac{\partial\tilde{\Theta}_{in}^{(1)}}{\partial\rho_j}\Big|_{\rho_j=\rho_{pj}} = \frac{\tilde{\Theta}_j^{(1)} - \tilde{\Theta}_{in}^{(1)}\Big|_{\rho_j=\rho_{pj}}}{R_{pj}}. \tag{24}$$

Also the prescribed heat injection rates per unit pipe length must be enforced onto the first order correction to the inner region. But their values $\tilde{q}_j$ have already been imposed onto the zeroth order solution obtained before. Consequently, the first order correction must have zero heat injection rates per unit pipe length so that its combination with the zeroth order solution still yields the prescribed values $\tilde{q}_j$:

$$0 = \int_{-\pi}^{\pi} -\kappa\frac{\partial\tilde{\Theta}_{in}^{(1)}}{\partial\rho_j}\Big|_{\rho_j=\rho_{pj}}\rho_{pj}\,d\theta_j.$$

Again, no exact solution to the formulated problem is known which does not pose a problem as only the general behavior of the first order correction in the ground is required. In this case, the general solution to the governing equation in the ground includes additional terms that represent the particular solution to the partial differential equation:

$$\tilde{\Theta}^{(1)}_{\text{in}}\Big|_{\rho\geq 1} = \tilde{A}_{10} + \tilde{B}_{10}\ln(\rho) + \sum_{\substack{n=-\infty\\ n\neq 0}}^{\infty}\left(\frac{\tilde{A}_{1n}}{\rho^{|n|}} + \rho^{|n|}\tilde{B}_{1n}\right)\mathrm{e}^{\imath n\theta} - \frac{\tilde{\mathrm{q}}}{4\pi}\left(\rho+\frac{1}{\rho}\right)\ln(\rho)\cos(\theta) + \sum_{\substack{n=-\infty\\ n\neq 0}}^{\infty}\frac{\tilde{A}_{0n}}{4}\left[\frac{\mathrm{e}^{\imath\frac{n}{|n|}(|n|+1)\theta}}{\rho^{|n|-1}} + \frac{\mathrm{e}^{\imath\frac{n}{|n|}(|n|-1)\theta}}{\rho^{|n|+1}}\right].$$

In the absence of thermal inertia, the heat injection rate per unit borehole length $\tilde{\mathrm{q}}$ coincides with the heat flux at the borehole wall integrated over the whole borehole wall. Substituting Eq. (10) into this condition leads to

$$\tilde{\mathrm{q}} = \int_{-\pi}^{\pi} -\frac{\partial\tilde{\Theta}^{(0)}_{\text{in}}}{\partial\rho}\Big|_{\rho=1}\mathrm{d}\theta + \mathrm{Pe}\int_{-\pi}^{\pi} -\frac{\partial\tilde{\Theta}^{(1)}_{\text{in}}}{\partial\rho}\Big|_{\rho=1}\mathrm{d}\theta + \mathcal{O}\left(\mathrm{Pe}^2\right).$$

Since the zeroth order solution already matches the value of $\tilde{\mathrm{q}}$, the first order correction must not contribute to this condition, a requirement that leads to the value of $\tilde{B}_{10}$:

$$0 = \int_{-\pi}^{\pi} -\frac{\partial\tilde{\Theta}^{(1)}_{\text{in}}}{\partial\rho}\Big|_{\rho=1}\mathrm{d}\theta \quad\rightarrow\quad \tilde{B}_{10} = \frac{\tilde{A}_{0(+1)} + \tilde{A}_{0(-1)}}{2}.$$

Finally, the first order correction to the fluid temperatures results from substituting Eqs. (10) and (11) into Eq. (6) and grouping the terms of order Pe:

$$\tilde{\Theta}^{(1)}_{j} = \frac{1}{2\pi}\int_{-\pi}^{\pi}\tilde{\Theta}^{(1)}_{\text{in}}\Big|_{\rho_j=\rho_{pj}}\mathrm{d}\theta_j. \tag{25}$$

3.4.2. Outer region

At distances from the borehole of order $\rho\sim 1/\mathrm{Pe}$, the velocity field is given by Eq. (17) which represents the only simplification made to the governing equation in the outer region. Since the terms being neglected in the velocity field are of order Pe^2, exactly the same partial differential equation results for the first order correction than for the zeroth order solution to the outer region:

$$s\,\tilde{\Theta}^{(1)}_{\text{out}} + \mathrm{Pe}\left[\cos(\theta)\frac{\partial\tilde{\Theta}^{(1)}_{\text{out}}}{\partial\rho} - \frac{\sin(\theta)}{\rho}\frac{\partial\tilde{\Theta}^{(1)}_{\text{out}}}{\partial\theta}\right] = \frac{1}{\rho}\frac{\partial}{\partial\rho}\left(\rho\frac{\partial\tilde{\Theta}^{(1)}_{\text{out}}}{\partial\rho}\right) + \frac{1}{\rho^2}\frac{\partial^2\tilde{\Theta}^{(1)}_{\text{out}}}{\partial\theta^2}.$$

Combined with the same homogeneous boundary condition at infinity, Eq. (7), the first order correction presents the same general expression as the zeroth order solution:

$$\tilde{\Theta}^{(1)}_{\text{out}} = \mathrm{e}^{\frac{\rho\mathrm{Pe}}{2}\cos(\theta)}\sum_{n=-\infty}^{\infty}\tilde{C}_{1n}\,K_n\left(\frac{\rho\mathrm{Pe}}{2}\sqrt{1+\frac{4s}{\mathrm{Pe}^2}}\right)\mathrm{e}^{\imath n\theta}.$$

3.4.3. Matching of both regions

The asymptotic matching between the inner and outer solutions is carried out again at an overlapping region located beyond the inner region but before the outer region. The differences between both solutions must be negligible there, a condition mathematically expressed as

$$\left(\tilde{\Theta}^{(0)}_{\text{in}} + \mathrm{Pe}\,\tilde{\Theta}^{(1)}_{\text{in}}\right)\Big|_{\rho\sqrt{\mathrm{Pe}}\gg 1} - \left(\tilde{\Theta}^{(0)}_{\text{out}} + \mathrm{Pe}\,\tilde{\Theta}^{(1)}_{\text{out}}\right)\Big|_{\rho\mathrm{Pe}\ll 1} \ll \mathrm{Pe}.$$

The zeroth order outer and inner solutions appear in the formulated condition as they contribute terms that need to be picked up by the first order corrections. So, the zeroth order outer solution, expanded for small values of $\rho\mathrm{Pe}$, introduces terms of order Pe:

$$\tilde{\Theta}^{(0)}_{\text{out}}\Big|_{\rho\mathrm{Pe}\ll 1} = \frac{\tilde{\mathrm{q}}}{2\pi}\left[1+\frac{\rho\mathrm{Pe}}{2}\cos(\theta)\right]\left[-\ln\left(\frac{\rho\mathrm{Pe}}{4}\sqrt{1+\frac{4s}{\mathrm{Pe}^2}}\right) - \gamma\right] + \mathcal{O}\left(\mathrm{Pe}^2\right).$$

These are matched to terms of the first order correction to the inner region. Some match without further intervention but others require their integration constants to be properly fixed:

$$\tilde{B}_{1(\pm1)} = \frac{\tilde{\mathrm{q}}}{8\pi}\left[-\ln\left(\frac{\mathrm{Pe}}{4}\sqrt{1+\frac{4s}{\mathrm{Pe}^2}}\right) - \gamma\right].$$

All other integration constants $\tilde{B}_{1n}$ are zero as no further positive powers of ρ exist among the leading terms of the expansion of the outer solution for small value of $\rho\mathrm{Pe}$.

Also the zeroth order inner solution introduces terms, that go as $1/\rho^{|n|}$, which need to be taken into account. In this case, by the first order correction to the outer region whose expansion for small values of $\rho\mathrm{Pe}$ is

$$\tilde{\Theta}^{(1)}_{\text{out}}\Big|_{\rho\mathrm{Pe}\ll 1} = \tilde{C}_{10}\left[-\ln\left(\frac{\rho\mathrm{Pe}}{4}\sqrt{1+\frac{4s}{\mathrm{Pe}^2}}\right) - \gamma + \mathcal{O}(\mathrm{Pe})\right] + \sum_{\substack{n=-\infty\\ n\neq 0}}^{\infty}\tilde{C}_{1n}\left[\left[1+\frac{\rho\mathrm{Pe}}{2}\cos(\theta)\right]\frac{2^{|n|-1}\,(|n|-1)!}{\left(\frac{\rho\mathrm{Pe}}{2}\sqrt{1+\frac{4s}{\mathrm{Pe}^2}}\right)^{|n|}} + \mathcal{O}\left(\mathrm{Pe}^{2-|n|}\right)\right]\mathrm{e}^{\imath n\theta}.$$

The outcome of the matching is

$$\tilde{C}_{1(\pm1)} = \frac{\tilde{A}_{0(\pm1)}}{2}\sqrt{1+\frac{4s}{\mathrm{Pe}^2}}.$$

All other integration constants $\tilde{C}_{1n}$ are zero as the matching requires them to be of order $\mathrm{Pe}^{|n|}$. Consequently, they do not belong to the level of approximation considered here. Nonetheless, setting $\tilde{C}_{1(\pm2)} = 0$ has some consequences for the performed matching process as it narrows the overlapping region. Since the corresponding unmatched terms in the zeroth order inner solution must be negligible in the overlapping region, it is necessary to ensure they are small compared to Pe. This leads to the following condition on ρ:

$$\frac{\tilde{A}_{0(\pm2)}}{\rho^2}\mathrm{e}^{\pm\imath 2\theta} \ll \mathrm{Pe} \quad\rightarrow\quad \rho \gg \frac{1}{\sqrt{\mathrm{Pe}}} \quad\leftrightarrow\quad \rho\sqrt{\mathrm{Pe}} \gg 1.$$

Finally, expressions for two additional integration constants are obtained from matching terms between the outer and inner solutions:

$$\tilde{C}_{10} = -\frac{\tilde{A}_{0(+1)} + \tilde{A}_{0(-1)}}{2},$$

$$\tilde{A}_{10} = \frac{\tilde{A}_{0(+1)} + \tilde{A}_{0(-1)}}{2}\left[\ln\left(\frac{\mathrm{Pe}}{4}\sqrt{1+\frac{4s}{\mathrm{Pe}^2}}\right) + \gamma + \frac{1}{2}\right].$$

In summary, the asymptotic matching between first order corrections to the inner and outer regions leads to the following final expressions for the first order corrections:

$$\tilde{\Theta}^{(1)}_{\text{in}}\Big|_{\rho\geq 1} = \tilde{A}_{10} + \tilde{B}_{10}\ln(\rho) + \sum_{\substack{n=-\infty\\ n\neq 0}}^{\infty}\frac{\tilde{A}_{1n}}{\rho^{|n|}}\mathrm{e}^{\imath n\theta} + \tilde{B}_{1(+1)}\rho\,\mathrm{e}^{+\imath\theta} + \tilde{B}_{1(-1)}\rho\,\mathrm{e}^{-\imath\theta} - \frac{\tilde{\mathrm{q}}}{4\pi}\left(\rho+\frac{1}{\rho}\right)\ln(\rho)\cos(\theta) + \sum_{\substack{n=-\infty\\ n\neq 0}}^{\infty}\frac{\tilde{A}_{0n}}{4}\left[\frac{\mathrm{e}^{\imath\frac{n}{|n|}(|n|+1)\theta}}{\rho^{|n|-1}} + \frac{\mathrm{e}^{\imath\frac{n}{|n|}(|n|-1)\theta}}{\rho^{|n|+1}}\right], \tag{26}$$

$$\tilde{\Theta}^{(1)}_{\text{out}} = \tilde{C}_{10}\,\mathrm{e}^{\frac{\rho\mathrm{Pe}}{2}\cos(\theta)}K_0\left(\frac{\rho\mathrm{Pe}}{2}\sqrt{1+\frac{4s}{\mathrm{Pe}^2}}\right) + \tilde{C}_{1(+1)}\,\mathrm{e}^{\frac{\rho\mathrm{Pe}}{2}\cos(\theta)}K_1\left(\frac{\rho\mathrm{Pe}}{2}\sqrt{1+\frac{4s}{\mathrm{Pe}^2}}\right)\mathrm{e}^{+\imath\theta} + \tilde{C}_{1(-1)}\,\mathrm{e}^{\frac{\rho\mathrm{Pe}}{2}\cos(\theta)}K_1\left(\frac{\rho\mathrm{Pe}}{2}\sqrt{1+\frac{4s}{\mathrm{Pe}^2}}\right)\mathrm{e}^{-\imath\theta}, \tag{27}$$

where for the sake of compactness the expressions for the integration constants have not been substituted.

4. Numerical examples

The capabilities and limitations of the developed model are demonstrated next by comparing its results against detailed numerical simulations of the unsteady heat transfer problem formulated in Section 2.2.

Since no exact expressions are available for the zeroth order inner solution and its first order correction, both are obtained numerically as well. On the contrary, the asymptotic solution to the outer region is known analytically, only requiring the values of $\tilde{A}_{0(\pm1)}$ to be obtained numerically.

4.1. Simulation procedure

All required numerical simulations are performed using the commercial software package COMSOL [63]. The convenience of COMSOL is that mathematical problems can be specified in a very precise way and without restrictions, even allowing the use of complex variables and arithmetic in the formulation and solution of problems.

4.1.1. Reference solution

The benchmark solution is obtained by directly solving the unsteady heat transfer problem formulated in Section 2.2. That is, Eqs. (8) and (9) for the unsteady thermal response of ground and grout, respectively, together with Eq. (7) for the boundary condition far from the borehole and Eq. (5) for the boundary condition at the pipe walls. Since heat injection rates per unit pipe length are enforced at each pipe, Eq. (6) is used to compute the corresponding fluid temperatures that appear in these boundary conditions at the pipe walls. Finally, the continuity conditions at the borehole wall, Eq. (4), are enforced automatically by COMSOL.

A sufficiently large computational domain, that spans till $\rho = 1000$, is defined in COMSOL so that truncation of the infinite ground has no negative consequences for the accuracy of the reference solution. And a sufficiently fine mesh, with the number of triangular elements ranging from 164,508 till 760,290 depending on the testcase, is used to ensure error levels below the threshold required by the present work.

4.1.2. Zeroth order solution to inner region

The zeroth order solution to the inner region is obtained by directly solving the mathematical problem formulated in Section 3.3.1. That is, Eq. (12) for the quasi-steady thermal response of grout and ground, the boundary condition at the pipe walls specified in Eq. (14), and the expression given in Eq. (16) for the fluid temperatures. As before, the continuity conditions in temperature and normal heat flux, Eq. (13), are enforced automatically by COMSOL.

Additionally, the asymptotic matching with the zeroth order solution to the outer region must be enforced as well in COMSOL. To do it, the behavior of the zeroth order inner solution far from the borehole, directly inferred from Eq. (19), is imposed as Dirichlet condition at a sufficiently large distance from the borehole:

$$\tilde{\Theta}_{\text{in}}^{(0)}\Big|_{\rho\gg1} = \frac{\tilde{\mathrm{q}}}{2\pi}\left[-\ln\left(\frac{\rho\mathrm{Pe}}{4}\sqrt{1+\frac{4s}{\mathrm{Pe}^2}}\right)-\gamma\right] + \sum_{\substack{n=-\infty\\ n\neq0}}^{\infty}\frac{\tilde{A}_{0n}}{\rho^{|n|}}\mathrm{e}^{\imath n\theta}.$$

The values of $\tilde{A}_{0n}$ with $n \neq 0$ need to be obtained from the numerical simulation itself. This is achieved by computing the Fourier series expansion of the numerical simulation at the borehole wall and then realizing that the resulting Fourier coefficients coincide with $\tilde{A}_{0n}$:

$$\tilde{A}_{0n} = \frac{1}{2\pi}\int_{-\pi}^{\pi}\tilde{\Theta}_{\text{in}}^{(0)}\Big|_{\rho=1}\mathrm{e}^{-\imath n\theta}\,\mathrm{d}\theta.$$

Only the lowest harmonics are actually required for the computations as their relevance decays rapidly with the size of the computational domain. Thus, for an outer radius of $\rho = 100$, as used here, the coefficients $\tilde{A}_{0(\pm1)}$ and $\tilde{A}_{0(\pm2)}$ are enough to exceed the desired accuracy level. Additionally, a fine mesh with a large number of triangular elements, between 46,208 and 1,068,172 depending on the testcase, is used as well to keep the discretization error below a certain threshold.

4.1.3. First order correction to inner region

The first order correction to the inner region is obtained by directly solving the mathematical problem formulated in Section 3.4.1. That is, Eq. (21) for the quasi-steady thermal response of the ground, for which the numerically-obtained zeroth order solution is required for the left hand side, Eq. (22) for the quasi-steady thermal response of the grout, Eq. (24) for the boundary condition at the pipe walls, and Eq. (25) for the fluid temperature in each pipe. Again, the enforcement of the continuity conditions at the borehole wall, Eq. (23), is done automatically by COMSOL.

As before, the asymptotic matching far from the borehole must be enforced as well in COMSOL. To do it, the behavior of the first order correction far from the borehole, directly inferred from Eq. (26), is imposed as Dirichlet condition at a sufficiently large distance from the borehole:

$$\begin{aligned}\tilde{\Theta}_{\text{in}}^{(1)}\Big|_{\rho\gg1} = {}& \frac{\tilde{A}_{0(+1)}+\tilde{A}_{0(-1)}}{2}\left[\ln\left(\frac{\rho\mathrm{Pe}}{4}\sqrt{1+\frac{4s}{\mathrm{Pe}^2}}\right)+\gamma+\frac{1}{2}\right]\\ &-\frac{\tilde{\mathrm{q}}}{4\pi}\rho\cos(\theta)\left[\ln\left(\frac{\rho\mathrm{Pe}}{4}\sqrt{1+\frac{4s}{\mathrm{Pe}^2}}\right)+\gamma\right]\\ &-\frac{\tilde{\mathrm{q}}}{4\pi}\frac{\ln(\rho)}{\rho}\cos(\theta)+\sum_{\substack{n=-\infty\\ n\neq0}}^{\infty}\frac{\tilde{A}_{1n}}{\rho^{|n|}}\mathrm{e}^{\imath n\theta}\\ &+\sum_{\substack{n=-\infty\\ n\neq0}}^{\infty}\frac{\tilde{A}_{0n}}{4}\left[\frac{\mathrm{e}^{\imath\frac{n}{|n|}(|n|+1)\theta}}{\rho^{|n|-1}}+\frac{\mathrm{e}^{\imath\frac{n}{|n|}(|n|-1)\theta}}{\rho^{|n|+1}}\right].\end{aligned}$$

Finally, the values of $\tilde{A}_{1n}$ are obtained in the same way as in the zeroth order solution to the inner region. The resulting expressions, however, are not that simple due to the particular solution to the governing equation in the ground:

$$\tilde{A}_{1(\pm1)} = \frac{1}{2\pi}\int_{-\pi}^{\pi}\tilde{\Theta}_{\text{in}}^{(1)}\Big|_{\rho=1}\mathrm{e}^{\mp\imath\theta}\,\mathrm{d}\theta - \frac{\tilde{A}_{0(\pm2)}}{4} + \frac{\tilde{\mathrm{q}}}{8\pi}\left[\ln\left(\frac{\mathrm{Pe}}{4}\sqrt{1+\frac{4s}{\mathrm{Pe}^2}}\right)+\gamma\right]$$

and, for $|n| \neq 1$,

$$\tilde{A}_{1n} = \frac{1}{2\pi}\int_{-\pi}^{\pi}\tilde{\Theta}_{\text{in}}^{(1)}\Big|_{\rho=1}\mathrm{e}^{-\imath n\theta}\,\mathrm{d}\theta - \frac{\tilde{A}_{0(n+1)}+\tilde{A}_{0(n-1)}}{4}.$$

Again, inclusion of the coefficients $\tilde{A}_{1(\pm1)}$ and $\tilde{A}_{1(\pm2)}$ is enough to exceed the desired accuracy level, and a large number of triangular elements, between 46,208 and 1,068,172 depending on the testcase, is used to keep the discretization error below a certain threshold.

4.1.4. Outer region

No numerical simulations are required to obtain the solution to the outer region as analytical expressions have been derived in the present work. Nonetheless, these expressions make use of the coefficients $\tilde{A}_{0(\pm1)}$ which are not known analytically. Hence, their values still need to be obtained from the numerical simulation performed in COMSOL for the zeroth order solution to the inner region.

To numerically evaluate the zeroth order solution and first order correction to the outer region, Eqs. (20) and (27) are implemented in Fortran95 using the algorithms developed by Zhang and Jin [64] for the computation of the modified Bessel functions of the second kind.

4.2. Borehole description

All presented comparisons use the borehole configuration depicted in Fig. 2. Although additional borehole configurations, with different geometrical and thermal characteristics as well as with coaxial and double U-shaped probes, have been analyzed, they are not discussed here as their results and conclusions are in line with the ones presented next.

The chosen configuration, whose geometrical and thermal characteristics are summarized in Table 2, consists in a borehole of diameter $2\,r_b = 152\,\text{mm}$ with two heterogeneous pipes inside. Pipe 1 has an outer diameter of $2\,r_{p1} = 40\,\text{mm}$ and a wall thickness of $d_1 = 3.7\,\text{mm}$. Pipe 2 presents an outer diameter of $2\,r_{p2} = 50\,\text{mm}$ and a wall thickness of $d_2 = 4.6\,\text{mm}$. Both pipes are placed at 5 mm from the borehole wall and

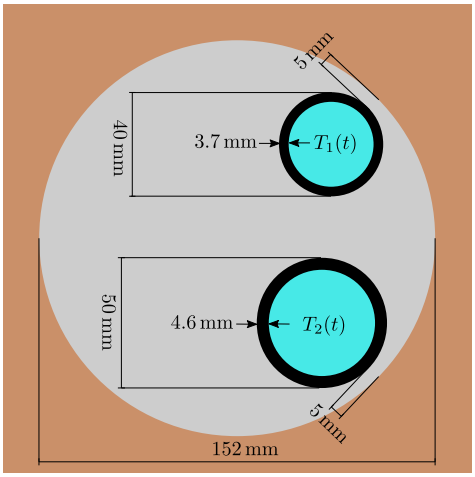

Fig. 2. Borehole configuration for the numerical examples.

at ±45° from the rear stagnation point. Hence, the polar coordinates of their centers are (51 mm, +45°) and (46 mm, −45°), respectively.

Both pipes are surrounded by a conventional grout of thermal conductivity $k_b = 1.50\,\mathrm{W/(m\,K)}$ [65] and thermal diffusivity $\alpha_b = 1.00 \cdot 10^{-7}\,\mathrm{m^2/s}$. Its thermal properties differ from the effective ones for the ground that are $k_g = 3.00\,\mathrm{W/(m\,K)}$ and $\alpha_g = 2.24 \cdot 10^{-7}\,\mathrm{m^2/s}$ [3].

Pure water is used as heat carrying liquid. Its density, specific heat capacity, thermal conductivity, and dynamic viscosity are $999\,\mathrm{kg/m^3}$, $4184\,\mathrm{J/(kg\,K)}$, $0.577\,\mathrm{W/(m\,K)}$, and $1.138 \cdot 10^{-3}\,\mathrm{kg/(m\,s)}$, respectively. A turbulent flow regime is ensured in both pipes by imposing a mass flow rate of $0.25\,\mathrm{kg/s}$. The corresponding convective heat transfer coefficients h_1 and h_2 are obtained using Gnielinski's correlations [66] which combined with the thermal conductivities of the pipes $k_1 = k_2 = 0.42\,\mathrm{W/(m\,K)}$ lead to the following values for the inner thermal resistances of the pipes:

$$R_{p1} = 0.535\,\frac{\mathrm{m\,K}}{\mathrm{W}}, \qquad R_{p2} = 0.544\,\frac{\mathrm{m\,K}}{\mathrm{W}}.$$

4.3. Solutions in the Laplace plane

The thermal interaction of the just-described borehole with a groundwater stream still has two unspecified parameters, namely, the Peclet number of the groundwater flow and the non-dimensional position s in the complex-valued Laplace plane. In the present section two different sets of values for Pe and s are considered. The first set serves to showcase the capabilities of the proposed asymptotic model while the second set highlights its limitations.

Additionally to Pe and s, time laws for the heat injection rates per unit pipe length are required as well. For the comparisons presented next, time-constant values are considered, namely, $\mathrm{q}_1(\tau) = 1$ and $\mathrm{q}_2(\tau) = 3$. Their Laplace transforms are $\tilde{\mathrm{q}}_1(s) = 1/s$ and $\tilde{\mathrm{q}}_2(s) = 3/s$, respectively.

4.3.1. $\mathrm{Pe} = 0.03$ *And* $s = (1+\imath)/2000$

Fig. 3 shows the grout/ground temperature for the favorable set of values for Pe and s. Modulus and argument of $\tilde{\Theta}$ are represented on the left and right plots, respectively, and three different solutions are compared in each plot. The reference solution is depicted using a solid color map, with the borehole wall and the two pipes marked by white circles. The zeroth order solution is represented using dashed red isolines and the complete asymptotic solution is drawn using solid black isolines.

The inner region, located at non-dimensional radial distances from the borehole of order unity, is shown at the top of Fig. 3. Since the zeroth order solution to the inner region completely neglects the convective transport of heat, it is concentric with respect to the pipes that act as heat sources in the problem. The first order correction, on the contrary, accounts for the convective transport of heat and, therefore, shifts the solution towards the right. Since the considered Peclet number is small, the observed shift is small as well.

The performance of the proposed model is very good, closely following the isolines for the modulus of the reference solution. In this sense, addition of the first order correction to the zeroth order solution clearly improves the accuracy of the model, which is best close to the borehole and inside the borehole.

The performance of the proposed model, however, is less good for the argument of the grout/ground temperature. There, the lack of thermal inertia in the mathematical problems defining the zeroth order solution and first order correction leads to a faster-than-necessary thermal response. Close to the borehole, as well as inside the borehole, the discrepancies are minimal and the proposed model performs well. But predicted values deviate significantly from the expected ones for increasing radial distances to the borehole.

The outer region, located at non-dimensional radial distances from the borehole of order $\rho \sim 1/\sqrt{|s|} \sim 40$, is shown at the middle of Fig. 3. In this case, the zeroth order solution and first order correction to the outer region must be used in the comparison with the reference solution.

While the zeroth order solution closely follows the modulus and argument isolines of the reference solution, the complete asymptotic solution directly overlaps them. The good performance of both approximation levels is explained by their mathematical problems. In both cases the simplified governing equation differs from the full equation only by terms in the velocity field that decay quadratically with ρ. Hence, both approximation levels are good representations of the full mathematical problem far from the borehole. Combined with the condensed, albeit valuable, information provided by the asymptotic matching with the inner region leads to the excellent results presented in Fig. 3.

Although not shown here, the accuracy of the proposed model far from the borehole is also outstanding for combinations of Pe and s that do not follow the distinguished limit $\mathrm{Pe} \sim \sqrt{|s|}$. This is so because the simplified governing equations defining the zeroth order solution and first order correction in the outer region include all three phenomena. That is, thermal inertia, heat convection, and heat conduction. Thus, when one phenomenon becomes dominant, the proposed model still represents it correctly.

Table 2
Geometrical and thermal characteristics of the borehole.

Variable	Value
Borehole diameter $2r_b$	152 mm
Grout thermal conductivity k_b	1.50 W/(m K)
Ground thermal conductivity k_g	3.00 W/(m K)
Grout thermal diffusivity α_b	$1.00 \cdot 10^{-7}\,\mathrm{m^2/s}$
Ground thermal diffusivity α_g	$2.24 \cdot 10^{-7}\,\mathrm{m^2/s}$
Water density	$999\,\mathrm{kg/m^3}$
Water specific heat capacity	4184 J/(kg K)
Water thermal conductivity	0.577 W/(m K)
Water dynamic viscosity	$1.138 \cdot 10^{-3}$ kg/(ms)
Pipe 1 outer diameter $2r_{p1}$	40 mm
Pipe 1 wall thickness d_1	3.7 mm
Pipe 1 wall thermal conductivity k_1	0.42 W/(m K)
Pipe 1 center radial coordinate	51 mm
Pipe 1 center angular coordinate	+45°
Pipe 1 mass flow rate	0.25 kg/s
Pipe 1 inner thermal resistance R_{p1}	0.535 m K/W
Pipe 2 outer diameter $2r_{p2}$	50 mm
Pipe 2 wall thickness d_2	4.6 mm
Pipe 2 wall thermal conductivity k_2	0.42 W/(m K)
Pipe 2 center radial coordinate	46 mm
Pipe 2 center angular coordinate	−45°
Pipe 2 mass flow rate	0.25 kg/s
Pipe 2 inner thermal resistance R_{p2}	0.544 m K/W

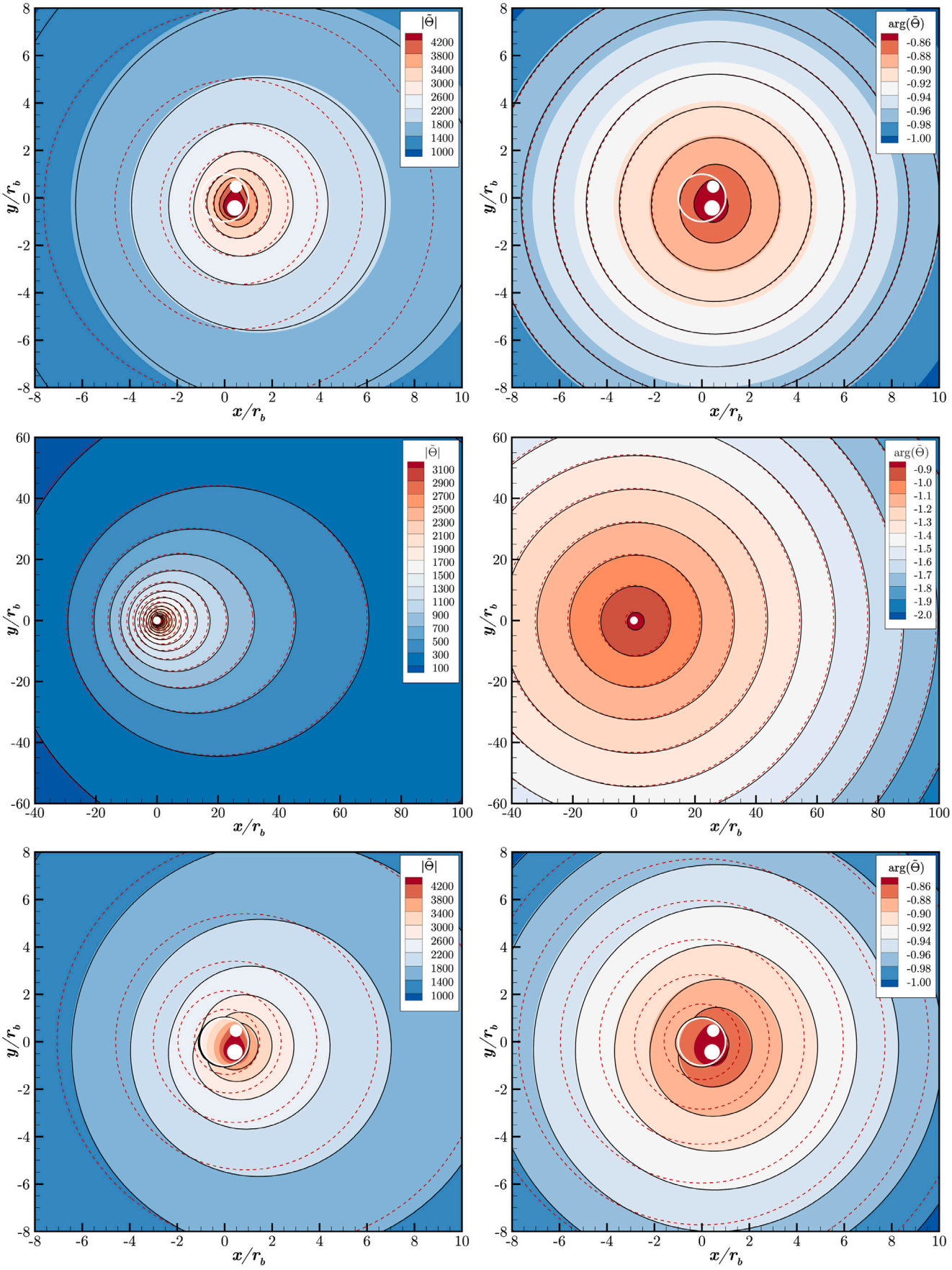

Fig. 3. (Top) inner solution, (middle) outer solution, and (bottom) outer solution close to the borehole for $\mathrm{Pe} = 0.03$ and $s = (1 + \imath)/2000$.

The solution to the outer region is meant to perform well at large distances from the borehole, as demonstrated in Fig. 3. Hence, good accuracy is not expected close to the borehole. Nonetheless, the solution to the outer region also performs well there, as shown at the bottom of Fig. 3. While the zeroth order solution to the outer region follows more or less the modulus and argument isolines of the reference solution, the complete asymptotic model follows them surprisingly good. In fact, better that the solution to the inner region presented before.

This *a-priori* unexpected accuracy is a consequence again of the presence of all three phenomena (thermal inertia, heat convection, and heat conduction) in the governing equations for the outer region. Then, the inner region can be seen as a simplified version of the outer region in which heat conduction dominates.

Of course, the outer solution is unable to represent the heat transfer taking place inside the borehole, reason why in the middle and bottom plots in Fig. 3 the dashed red isolines and black isolines end at the borehole wall. Additionally, the outer solution requires information from the inner solution to correctly set the values of its integration constants $\tilde{C}_{00}$, $\tilde{C}_{10}$, and $\tilde{C}_{1(\pm1)}$. Hence, an inner region with its asymptotic solution is always required regardless of the performance of the outer solution close to the borehole.

4.3.2. Pe = 1.00 *And* $s = (1 + \imath)/2000$

When the Peclet number of the groundwater flow or the non-dimensional position s in the complex-valued Laplace place are not small compared to unity, the premise for the performed asymptotic analysis no longer exists. Then, the proposed model looses its validity and a sharp drop in its accuracy is expected.

Fig. 4 shows the grout/ground temperature for the unfavorable set of values of Pe = 1.00 and $s = (1 + \imath)/2000$. Again, modulus and argument of $\tilde{\Theta}$ are represented on the left and right plots, respectively, and three different solutions are compared in each plot using the same representation convention as in the previous subsection.

As anticipated, the proposed model fails to correctly reproduce the temperature distribution in grout and ground. In fact, only the modulus of the grout temperature is predicted reasonably well. Everything else presents unacceptable error levels. Also the addition of the first order correction to the zeroth order solution, which in the previous example improved the results, does not help in this case.

Despite the bad results close to the borehole, the proposed model performs surprisingly well further away from the borehole, at the outer region. As seen in Fig. 4, it correctly reproduces there the modulus and argument of the ground temperature. Again, this is a consequence of two factors. First, that all three phenomena (thermal inertia, heat convection, and heat conduction) are present in the governing equations for the outer region. Second, that the solution to the inner region is accurate enough at the borehole wall, where the values of $\tilde{A}_{0n}$ are defined, so that the integration constants $\tilde{C}_{00}$, $\tilde{C}_{10}$, and $\tilde{C}_{1(\pm1)}$ are accurate as well.

The solution to the outer region also performs well close to the borehole, as observed at the bottom of Fig. 4. In fact, it clearly outperforms the solution to the inner region presented before. This casts again doubts on the need and usefulness of the inner region. But as already pointed out in the previous example, the inner region is integral part of the asymptotic analysis leading to the proposed model so that it cannot be obviated or circumvented.

Although not shown here, the same conclusions regarding the performance of the proposed model apply to other combinations of unfavorable values for Pe and s. For instance, small Peclet numbers combined with order unity values of s. Or Peclet numbers and values of s that are both of order unity. In all these cases the proposed model performs well far from the borehole but fails to correctly reproduce the temperature field inside the borehole and close to it.

4.4. Solutions in the time domain

Known the grout/ground temperature in the complex-valued Laplace plane, the time evolution of the problem is recovered by applying the inverse Laplace transform. Due to the mathematical complexity of the developed model, this step is done numerically [67]. The algorithm to use requires the evaluation of the solution at a reduced set of positions s in the Laplace plane. The computation of these solutions as well as the subsequent application of the inversion algorithm is performed entirely within COMSOL.

The computational cost of the followed approach is lower than the one of time-marching the governing equations till the time instants of interest. For the two examples shown next, for which the complete grout/ground temperatures are required, a threefold speedup is achieved. Also overall grid independence is accomplished much easier for this unsteady problem as temporal discretization errors are nonexistent and the accuracy of the numerical inversion of the Laplace transform is on par with machine precision [67].

4.4.1. Pe = 0.03

Fig. 5 shows the time evolution of the grout/ground temperature for the favorable Peclet number of 0.03. Three different instants in time are shown, namely, $\tau = 20$ at the top, $\tau = 200$ at the middle, and $\tau = 2000$ at the bottom. The left and right plots represent, respectively, the inner and outer solutions using the same representation convention as in previous figures, with the reference solution included as well in the plots.

One of the hypotheses underlying the asymptotic analysis of the present work is that the characteristic heat injection time t_q is large compared to the characteristic transversal diffusion time t_b. This requires the non-dimensional time τ to be large compared to unity for the developed model to perform well. The results shown in Fig. 5 confirm this. The shown results also reveal that the model performs well for the not-so-large value of $\tau = 20$, especially the asymptotic solution to the outer region.

To quantitatively assess the accuracy of the proposed model, Fig. 6 represents, for $\tau = 2000$, the different solutions along the green line depicted in Fig. 5. This line starts at the rear stagnation point of the borehole, located at $(r, \theta) = (r_b, 0°)$, and follows the groundwater flow downstream of the borehole. The left plot in Fig. 6 represents the temperatures attained by the reference solution and by the different asymptotic solutions for the inner and outer regions. The right plot represents the absolute errors of the different asymptotic solutions when compared to the reference solution.

Close to the borehole, the zeroth order solution to the inner region follows the reference solution with absolute (relative) errors in the range of 0.03–0.20 (1.1%–15.4%). The accuracy improves an order of magnitude by adding the first order correction to the inner region, leading to absolute (relative) errors in the range of 0.002–0.03 (0.1%–2.3%). As expected, the obtained solutions for the inner region perform worse with increasing distances from the borehole, where the solutions to the outer region must be used instead.

Far from the borehole, the zeroth order solution to the outer region already performs good, with absolute (relative) errors that start at 0.03 (2.3%) and decay with increasing distances to the borehole. Inclusion of the first order correction to the outer region improves again the accuracy by an order of magnitude, leading to absolute (relative) errors below 0.002 (0.2%). The complete asymptotic solution to the outer region also performs good at distances to the borehole belonging to the inner region of the problem: The crossover between the outer and inner solutions takes place at non-dimensional distances between 3 and 4.

To ensure the correctness of the absolute errors shown in Fig. 6, successive mesh refinements were performed in COMSOL till the plotted curves stopped changing. Fig. 7 exemplifies this by showing the evolution of the reference temperature at the rear stagnation point of the borehole, located at $(r, \theta) = (r_b, 0°)$, with the number of mesh nodes.

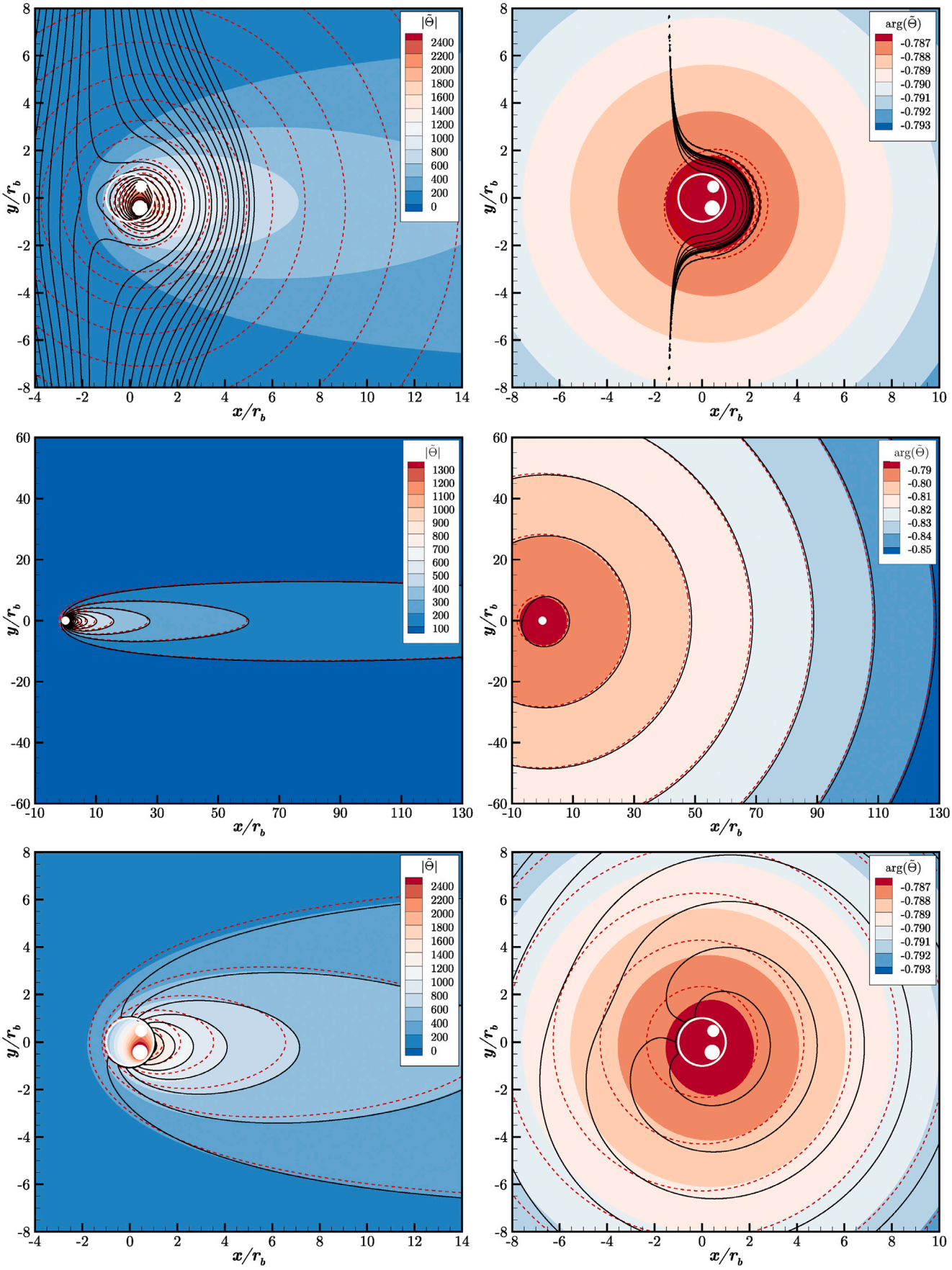

Fig. 4. (Top) inner solution, (middle) outer solution, and (bottom) outer solution close to the borehole for Pe = 1.00 and $s = (1 + \imath)/2000$.

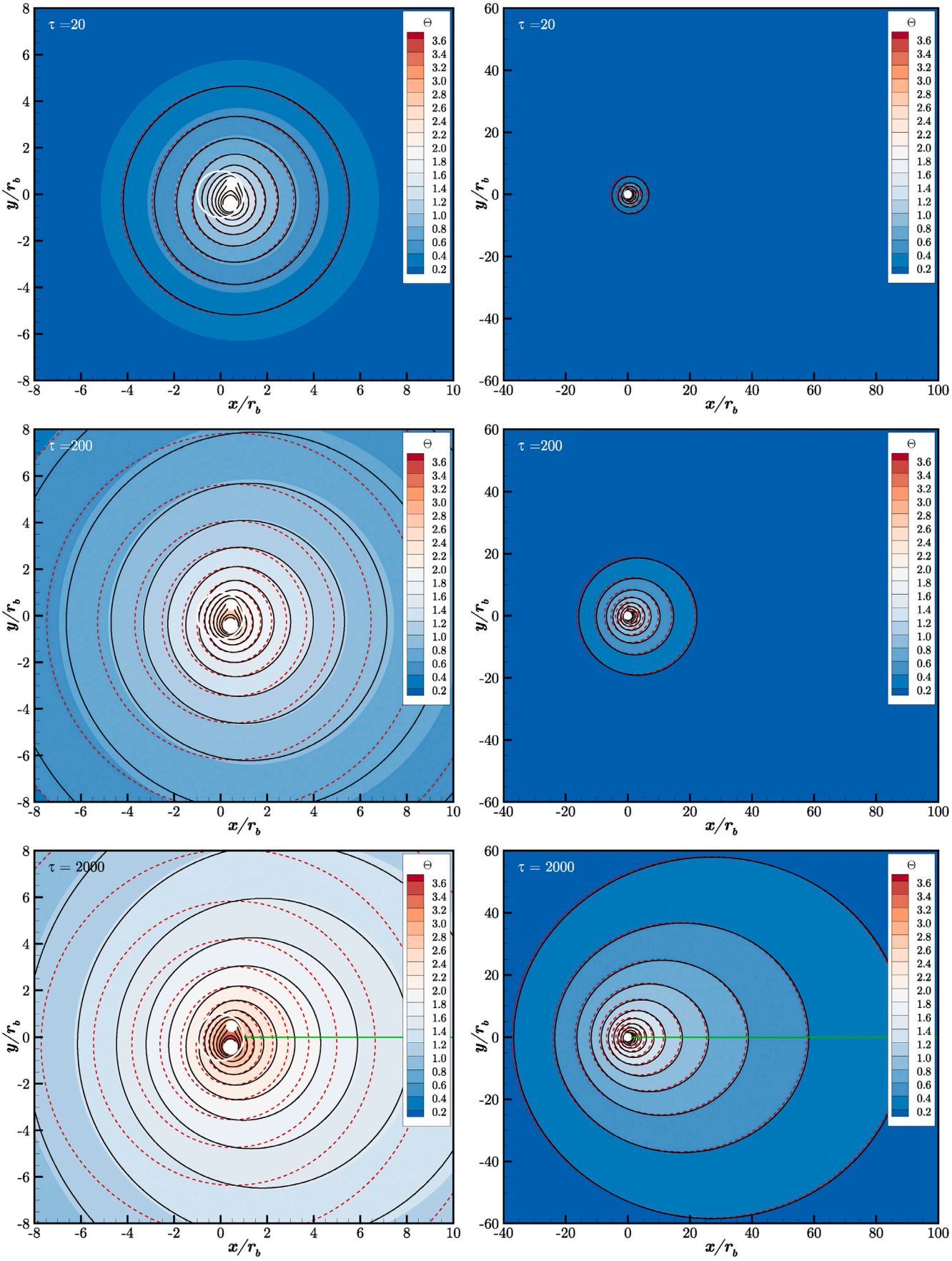

Fig. 5. (Left) inner solution and (right) outer solution for Pe = 0.03.

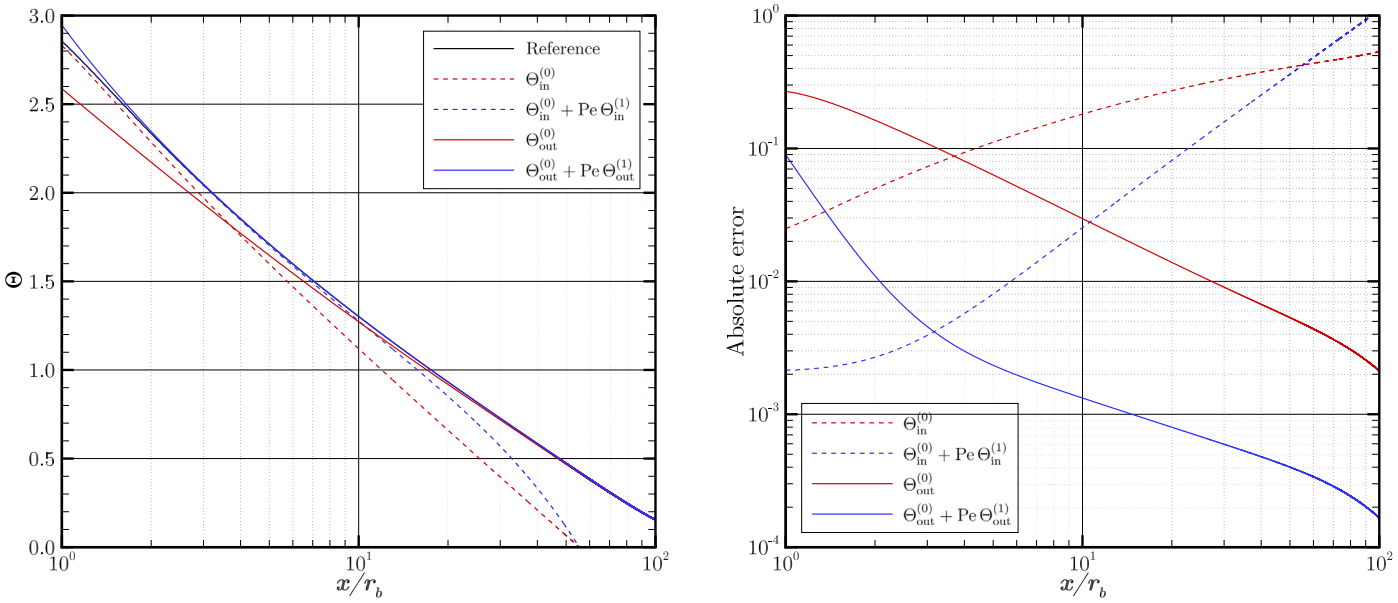

Fig. 6. (Left) Temperature and (right) absolute errors for Pe = 0.03 and $\tau = 2000$.

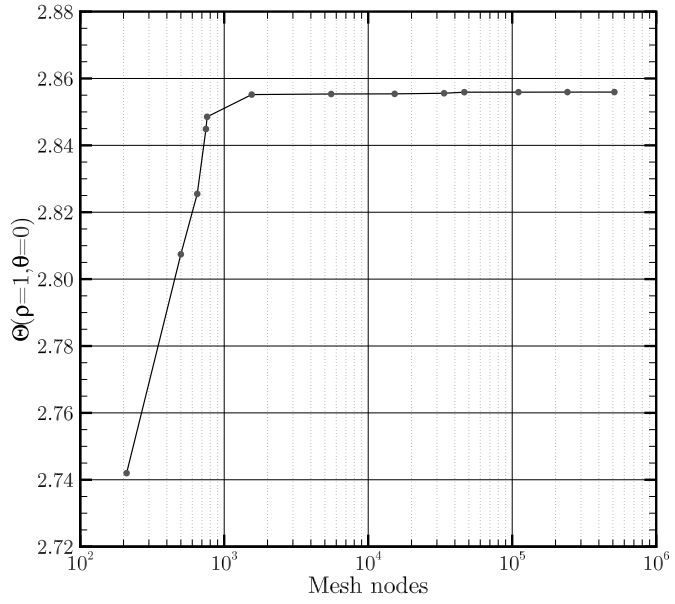

Fig. 7. Rear stagnation point temperature versus number of mesh nodes.

4.4.2. Pe = 1.00

Fig. 8 shows the time evolution of the grout/ground temperature for the unfavorable Peclet number of 1.00 using the same representation convention as before. Three different instants in time are shown, namely, $\tau = 20$ at the top, $\tau = 50$ at the middle, and $\tau = 200$ at the bottom.

Since the convective transport of heat is now stronger, the thermal wake behind the borehole builds up faster so that the final steady-state is already attained for $\tau = 200$. The steady-state is reached even sooner close to the borehole, where no relevant differences can be observed between the grout/ground temperatures at $\tau = 50$ and $\tau = 200$.

Regarding the performance of the proposed model, all remarks made so far also apply to this case so that its inclusion is more for the sake of completeness than for the discussion of anything new.

4.5. Time-harmonic responses

So far, the problem has been addressed in the complex-valued Laplace plane. This is of great practical interest as it allows arbitrarily-varying heat injection rates per unit pipe length to be specified at the pipes. More enlightening, however, is the analysis of the thermal response to time-harmonic variations as then a sweep in angular frequencies can be performed. This sweep allows to show and discuss the rise and fall of thermal inertia with the aid of one single plot. As shown next, the proposed model is also applicable, with a minor tweak, to this case [53].

Consider the following time-harmonic variations for the grout/ground temperature, for the fluid temperatures in the pipes, for the heat injection rates per unit pipe length, and for the heat injection rate per unit borehole length:

$$\Theta = \hat{\Theta}\,e^{\imath\omega\tau} + \hat{\Theta}^*\,e^{-\imath\omega\tau}, \qquad \Theta_j = \hat{\Theta}_j\,e^{\imath\omega\tau} + \hat{\Theta}_j^*\,e^{-\imath\omega\tau},$$
$$q_j = \hat{q}_j\,e^{\imath\omega\tau} + \hat{q}_j^*\,e^{-\imath\omega\tau}, \qquad q = \hat{q}\,e^{\imath\omega\tau} + \hat{q}^*\,e^{-\imath\omega\tau}.$$

In these expressions ω is the non-dimensional angular frequency of the time-harmonic variations, $\hat{\Theta}$, $\hat{\Theta}_j$, $\hat{q}_j$, and $\hat{q}$ are the corresponding harmonics, and the superscript * denotes the complex conjugate of a variable.

Substitution of these time-harmonic variations into the heat transfer problem formulated in Section 2 leads to a mathematical problem for the harmonics $\hat{\Theta}$ and $\hat{\Theta}_j$ that is almost identical to the one for the Laplace-transformed functions $\tilde{\Theta}$ and $\tilde{\Theta}_j$. Only the governing equations in ground and grout change slightly, being now

$$\imath\omega\,\hat{\Theta} + \mathrm{Pe}\left[v_\rho\frac{\partial\hat{\Theta}}{\partial\rho} + \frac{v_\theta}{\rho}\frac{\partial\hat{\Theta}}{\partial\theta}\right] = \frac{1}{\rho}\frac{\partial}{\partial\rho}\left(\rho\frac{\partial\hat{\Theta}}{\partial\rho}\right) + \frac{1}{\rho^2}\frac{\partial^2\hat{\Theta}}{\partial\theta^2}$$

and

$$\imath\omega\frac{\alpha_g}{\alpha_b}\hat{\Theta} = \frac{1}{\rho}\frac{\partial}{\partial\rho}\left(\rho\frac{\partial\hat{\Theta}}{\partial\rho}\right) + \frac{1}{\rho^2}\frac{\partial^2\hat{\Theta}}{\partial\theta^2}.$$

Thus, all formulae derived in Section 3 is also applicable to time-harmonic problems once position s is replaced by $\imath\omega$. The same applies to the thermal influence of the borehole discussed later in Section 7.

The frequency response of the borehole and its surrounding ground is presented in Fig. 9. The left and right plots show the modulus and argument of the mean azimuthal borehole wall temperature $\hat{\Theta}_b$, respectively, as returned by the reference solution, by the zeroth order solution, and by the complete asymptotic solution.

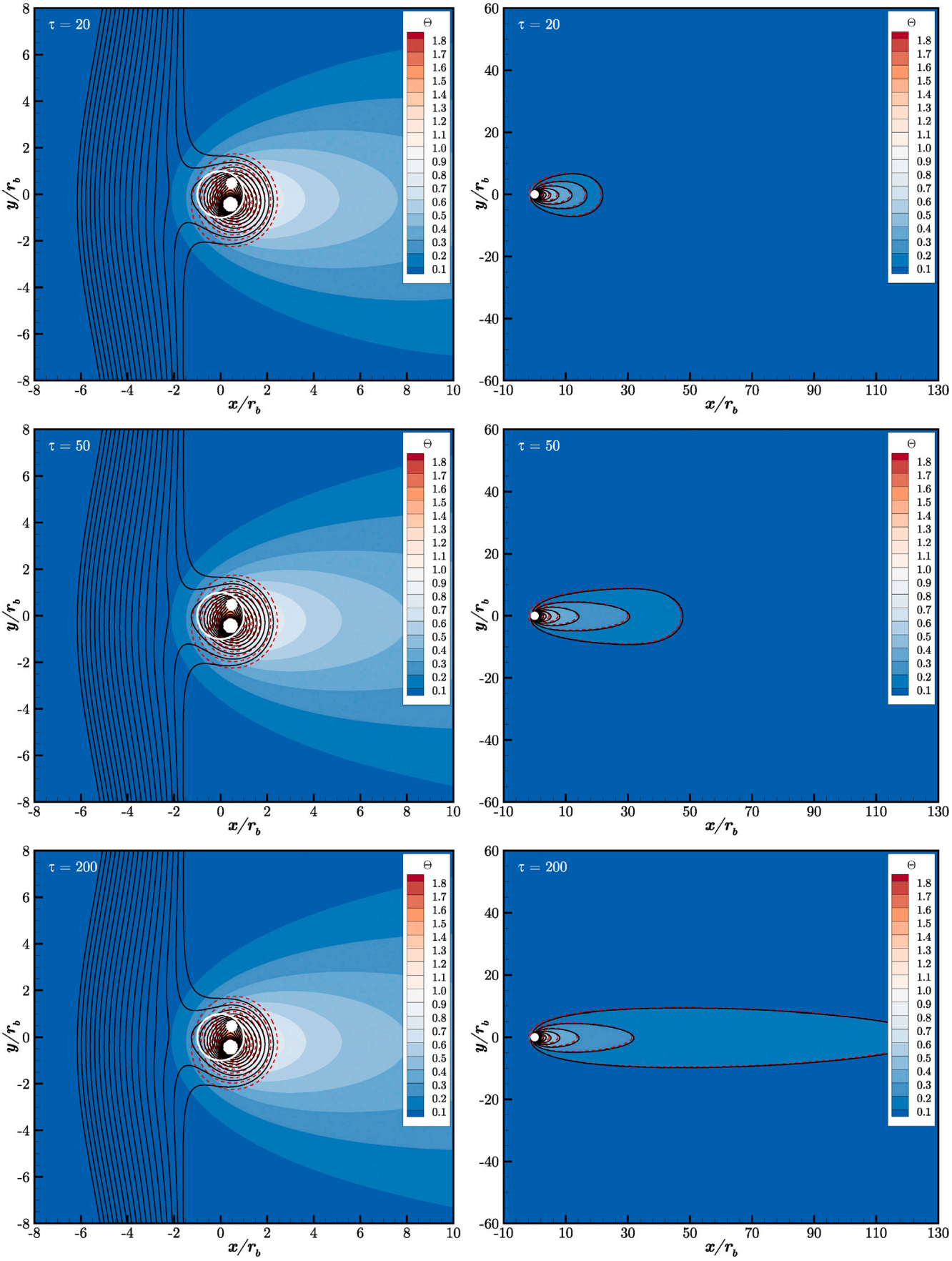

Fig. 8. (Left) inner solution and (right) outer solution for Pe = 1.00.

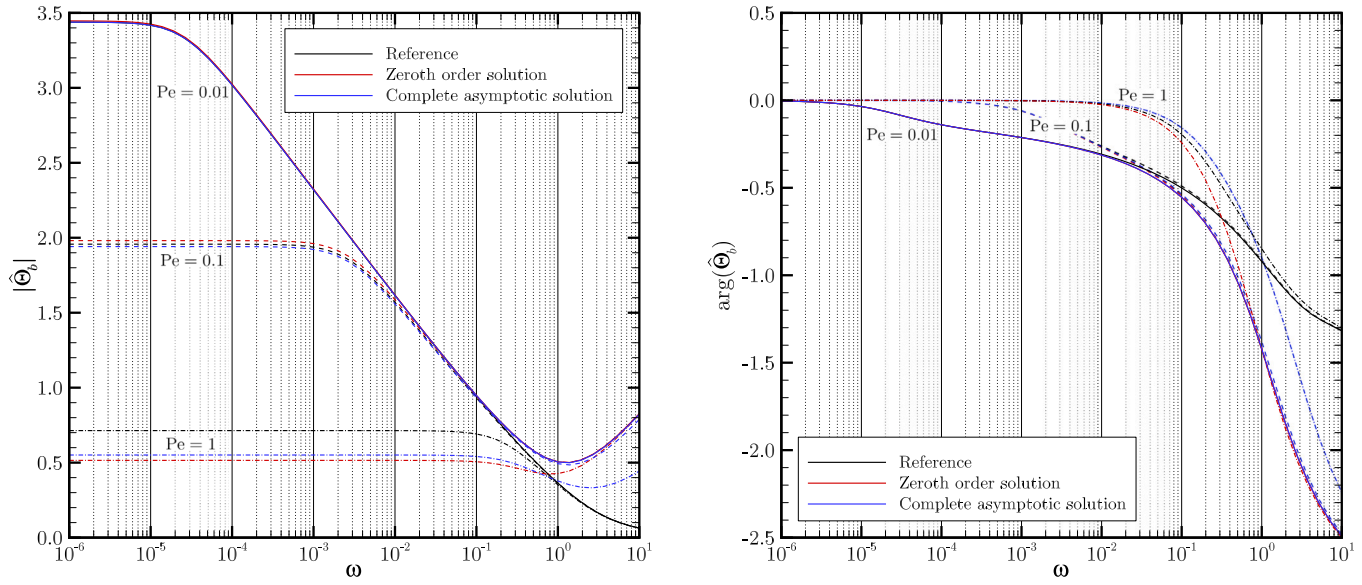

Fig. 9. Mean azimuthal borehole wall temperature $\hat{\Theta}_b$.

The represented temperature $\hat{\Theta}_b$, defined as

$$\hat{\Theta}_b = \frac{1}{2\pi}\int_{-\pi}^{\pi} \hat{\Theta}\Big|_{\rho=1} \mathrm{d}\theta,$$

is considered by most researchers as the temperature at which the borehole perceives the surrounding ground [18]. This interpretation, however, is known to be flawed in the absence of groundwater flows [51,53]. But the momentary lack of a better alternative, as explained later in Section 6, renders it as the best available quantity to represent here.

For values of the Peclet number of order 0.01, the proposed model accurately reproduces the mean azimuthal borehole wall temperature $\hat{\Theta}_b$, with the three curves for the reference solution, the zeroth order solution, and the complete asymptotic solution being almost indistinguishable in the plots.

The three curves become distinguishable for Peclet numbers an order of magnitude larger. That is, for $\mathrm{Pe} \sim 0.1$. But the accuracy of the proposed model remains high, with relative errors below 1% for the modulus of $\hat{\Theta}_b$. It is not until Peclet numbers of order unity that the relative errors reach unacceptable levels of almost 23%. This makes sense as the performed asymptotic analysis is not valid for such large values of the Peclet number and, consequently, the accuracy of the proposed model cannot be assured.

The previous accuracy assessments and discussions hold as long as the non-dimensional angular frequency ω is small compared to unity. Then, the characteristic time t_q of the harmonic oscillation, closely related to its period, is large compared to the characteristic transversal diffusion time t_b and the performed asymptotic analysis is valid. Therefore, it comes as no surprise that the proposed model fails to correctly predict the mean azimuthal borehole wall temperature $\hat{\Theta}_b$ for non-dimensional angular frequencies of order unity.

In summary, the numerical examples presented and discussed show that the proposed model performs well as long as the underlying asymptotic analysis is valid. That is, as long as the Peclet number of the groundwater flow is small compared to unity and the characteristic heat injection time t_q is large compared to the characteristic transversal diffusion time t_b. If these conditions are not met, the proposed model fails to correctly represent the grout/ground temperature in the vicinity of the borehole, although it still succeeds in reproducing the ground temperature further away from the borehole.

5. Existing models for the problem

Most models for the thermal response of geothermal boreholes do not consider the presence of aquifers. For them, conduction is the solely heat transfer mechanism in the ground. Although apparently unrelated to the present work, these models are responsible for most of the characteristics of the models to review. Therefore, the discussion that follows next inevitably starts with them.

A common denominator to most models involving purely-conducting grounds is that the characteristic heat injection time t_q is considered large compared to the characteristic transversal diffusion time t_b [29,41,47,53]. This assumption introduces a two-region structure into the problem that enables the development of efficient, albeit accurate, theoretical models for the thermal response of geothermal boreholes [13].

The inner region, located close to the borehole, is quasi-steady. In the case of purely-conducting grounds, its solution leads to a highly convenient network of thermal resistances that links the heat injection rates per unit pipe length of the pipes with certain temperature differences [47,53,58,59].

One of the temperatures involved represents the thermal behavior of the ground located further away from the borehole. To obtain its value, the solution to the unsteady outer region, located beyond the inner region, is required. That solution is usually obtained by superposition of point sources of heat that represent the thermal influence of the borehole onto the purely-conducting ground [19,29,68].

The average temperature of the outer solution at the borehole wall, known as the mean azimuthal borehole wall temperature [47], is considered by most researchers as the temperature representing the thermal behavior of the ground located further away from the borehole [13,29,59,69]. In the limit of slowly-varying heat injection rates, for which $t_q \gg t_b$, this assumption is correct [47,51,53]. The same does not hold, though, for other relationships between t_q and t_b [51,53].

Adding an aquifer to the ground significantly changes the heat transfer problem to solve. Hence, ideas, concepts, and modeling approaches meant for purely-conducting grounds do not necessarily extrapolate to the thermal interaction of geothermal boreholes with groundwater flows. Nonetheless, researchers have assumed they are applicable and have developed successful models that present the very same features [17,18]. A formal proof that this can be done, at least for creeping groundwater flows, was not available until the present work and the follow-up one [70].

So, models involving groundwater flows present two distinct regions. The inner region, located close to the borehole, is quasi-steady and heat conduction is the only heat transfer mechanism in it. The outer region, located further away from the borehole, is unsteady

and considers both heat transfer mechanisms in the ground, namely, conduction and convection, with the latter one slightly simplified due to the assumption of a uniform velocity for the groundwater stream. Finally, both regions are interweaved through the mean azimuthal borehole wall temperature.

By comparing the described model structure with the present work it becomes evident that the state of the art corresponds to the zeroth order solution of the proposed model, with the integration constant $\tilde{A}_{00}$ embodying the mean azimuthal borehole wall temperature.

Most reviewed models obtain the solution to the outer region by superposing moving point-sources of heat that represent the thermal influence of the borehole onto a ground moving at the effective seepage velocity U_∞ [19]. If the borehole is assumed infinitely long, the so-called *moving infinite line source models* result [14,20–25]. On the contrary, the *moving finite line source models* take into account the finite length of the borehole [24–36].

Moving infinite line source models are meant, just as the model proposed in the present work, for operating conditions of the borehole in which the characteristic heat injection time t_q is small compared to the characteristic longitudinal diffusion time t_H. Then, three-dimensional effects at the borehole endings are not important and the finite length of the borehole plays a secondary role in the thermal response of the ground [45,47].

Moving finite line source models, on the contrary, take into account the finite length of the borehole and the aforementioned three-dimensional effects at the borehole endings. Consequently, they are also valid for operating conditions in which t_q and t_H are comparable in order. A downside of these models, however, is the significant increase in mathematical complexity and computational cost. To partially mitigate this, all moving finite line source models assume a uniform heat injection rate per unit borehole length q along the borehole. For purely-conducting grounds, however, it is known that this simplification is not correct [48,49,52]. Nonetheless, good results for the thermal response of geothermal boreholes are obtained with it [46].

Another simplification made by most moving finite line source models is to assume groundwater flows with the same effective seepage velocity U_∞ at all depths. This hypothesis oversimplifies the strata structure of the ground in which aquifers are confined to certain depth ranges and are surrounded by purely-conducting layers of rock or soil. Only the models developed by Hu [31] and by Erol and François [27] take into account the layered structure of aquifers, although they do it a clumsy way.

A different approach to the thermal response of the ground is offered by *infinite cylindrical source models*. These take into account the finite radius of the borehole when solving the heat transfer problem in the ground, a task accomplished either numerically [4,39,40] or analytically [37,38]. Inclusion of the borehole radius is considered an improvement over models based on point-sources of heat. However, the present work shows that the improvement must be rather small as neither the zeroth order solution nor the first order correction to the outer region depend explicitly on the borehole radius (ρPe and s/Pe^2 do not depend on r_b). Consequently, its effect is relegated to the integration constants $\tilde{A}_{0(\pm1)}$, present in $\tilde{C}_{10}$ and $\tilde{C}_{1(\pm1)}$, and to higher order terms of the asymptotic expansion of the problem. Additionally, infinite cylindrical source models introduce important simplifications in order to account for the borehole radius. So, all reviewed models replace the interior of the borehole by a uniform Dirichlet or Neumann boundary condition at the borehole wall [4,37–40]. And some assume as well the groundwater flow to be uniform everywhere, a simplification incompatible with the very presence of the borehole in the ground [37,38].

Finally, hybrid models do exist as well that use all described modeling approaches [41–44]. They choose one approach or the other depending on the value attained by the characteristic heat injection time t_q. This renders them more complex but also more efficient from a computational point of view.

6. Apparent temperature of the ground

The grout/ground temperature derived in Section 3, although essential, is not the quantity of interest for the analysis of the thermal response of geothermal boreholes. What is relevant instead is how the perturbed grout/ground temperature appears in the governing equations for the convective transport of heat along the pipes, and whose solution represents the sought thermal response of the borehole.

In the absence of groundwater flows everything is well understood. All effects of the perturbed grout/ground temperature condense into one single quantity called the apparent temperature of the ground [47,53]. This temperature differs from the unperturbed one, T_∞, in the thermal influence the borehole exerts onto itself as a consequence of the continuous exchange of heat with the ground. Therefore, it represents the temperature at which the borehole perceives the surrounding ground and is, as such, the same for all pipes. The derivation of mathematical expressions for it represents an essential aspect of the modeling of the thermal response of geothermal boreholes [47–49,52].

In the presence of groundwater flows, through, the applicability of the aforementioned concept is not assured. First and foremost, the enhanced multipole method used for the rigorous solution of the heat conduction problem in grout and ground does not account for groundwater flows [53]. Hence, the resulting mathematical proof and physical interpretation of the apparent temperature of the ground do not necessarily extend to boreholes interacting with groundwater flows. Second, the moving groundwater introduces an asymmetry into the problem. This casts doubts on the spatial uniformity of the apparent temperature of the ground meaning that different pipes in a borehole could perceive the surrounding ground in different ways.

The answer to all these doubts is beyond the scope of the present work as the exact solution to the formulated heat transfer problem is required for that. Only so is it possible to correctly identify what precisely is the apparent temperature of the ground. The authors have addressed this challenge by modifying the enhanced multipole method [70]. However, not the full heat transfer problem formulated in Section 2 has been considered for that but the asymptotic approach presented in Section 3. The outcome of their work is that an apparent temperature of the ground can still be defined in the presence of creeping groundwater flows, but different values result for each pipe in the borehole.

7. Thermal influence of a borehole

The thermal interaction between adjacent boreholes has negative consequences for the performance of geothermal HVAC systems. Hence, the thermal influence exerted by a geothermal borehole onto its surrounding ground is of utmost importance for the accurate forecasting of the thermal response of geothermal heat exchangers composed of multiple boreholes.

The typical distance between adjacent boreholes, of a few meters, is significantly larger than the borehole radius so that $\rho \gg 1$. Consequently, the solution to the outer region is employed to describe the thermal influence a certain borehole exerts onto adjacent boreholes. By truncating the asymptotic expansion for the outer solution, Eq. (10), and substituting thereafter the derived expressions for the zeroth order solution and first order correction:

$$\begin{aligned}\tilde{\Theta}_{\mathrm{out}} = &\left[\frac{\tilde{\mathrm{q}}}{2\pi} + \mathrm{Pe}\,\tilde{C}_{10}\right] \mathrm{e}^{\frac{\rho\mathrm{Pe}}{2}\cos(\theta)} K_0\left(\frac{\rho\mathrm{Pe}}{2}\sqrt{1+\frac{4s}{\mathrm{Pe}^2}}\right)\\ &+ \mathrm{Pe}\,\tilde{C}_{1(+1)}\,\mathrm{e}^{\frac{\rho\mathrm{Pe}}{2}\cos(\theta)} K_1\left(\frac{\rho\mathrm{Pe}}{2}\sqrt{1+\frac{4s}{\mathrm{Pe}^2}}\right)\mathrm{e}^{+\imath\theta}\\ &+ \mathrm{Pe}\,\tilde{C}_{1(-1)}\,\mathrm{e}^{\frac{\rho\mathrm{Pe}}{2}\cos(\theta)} K_1\left(\frac{\rho\mathrm{Pe}}{2}\sqrt{1+\frac{4s}{\mathrm{Pe}^2}}\right)\mathrm{e}^{-\imath\theta}.\end{aligned}$$

Replacing the integration constants $\tilde{C}_{10}$ and $\tilde{C}_{1(\pm1)}$ by their expressions leads, after some rearrangement, to

$$\tilde{\Theta}_{\mathrm{out}} = \frac{\tilde{\mathrm{f}}}{2\pi}\,\mathrm{e}^{\frac{\rho\mathrm{Pe}}{2}\cos(\theta)} K_0\left(\rho\sqrt{s+\frac{\mathrm{Pe}^2}{4}}\right)$$

$$+\ \tilde{A}_{0(+1)}\,\mathrm{e}^{\frac{\rho\mathrm{Pe}}{2}\cos(\theta)}\sqrt{s+\frac{\mathrm{Pe}^2}{4}}\,K_1\left(\rho\sqrt{s+\frac{\mathrm{Pe}^2}{4}}\right)\mathrm{e}^{+\imath\theta}$$
$$+\ \tilde{A}_{0(-1)}\,\mathrm{e}^{\frac{\rho\mathrm{Pe}}{2}\cos(\theta)}\sqrt{s+\frac{\mathrm{Pe}^2}{4}}\,K_1\left(\rho\sqrt{s+\frac{\mathrm{Pe}^2}{4}}\right)\mathrm{e}^{-\imath\theta}. \tag{28}$$

A non-dimensional fictitious heat injection rate per unit borehole length $\tilde{\mathrm{f}}$ is identified in the previous expression. It subtracts from the true value $\tilde{\mathrm{q}}$ the contributions of the azimuthal corrections:

$$\tilde{\mathrm{f}}(s)=\tilde{\mathrm{q}}(s)-\mathrm{Pe}\,\pi\big(\tilde{A}_{0(+1)}(s)+\tilde{A}_{0(-1)}(s)\big).$$

To complete the formulae for the thermal influence of a borehole, expressions for $\tilde{A}_{0(\pm1)}$ are required. As shown in Hermanns and Rivero [51] and Rico and Hermanns [70], they are linear combinations of the heat injection rates per unit pipe length $\tilde{\mathrm{q}}_j$, with the weights not depending on the position s in the complex-valued Laplace plane:

$$\tilde{A}_{0n}(s)=\sum_{j=1}^{N_p}A_{0nj}\,\frac{\tilde{\mathrm{q}}_j(s)}{2\pi\kappa}.$$

In the absence of an exact expression for the zeroth order solution to the inner region, as happens in the present work, the coefficients $\tilde{A}_{0(\pm1)}$ are obtained numerically following the same procedure as in Section 4:

$$\tilde{A}_{0(\pm1)}(s)=\frac{1}{2\pi}\int_{-\pi}^{\pi}\tilde{\Theta}^{(0)}_{\mathrm{in}}\Big|_{\rho=1}\mathrm{e}^{\mp\imath\theta}\,\mathrm{d}\theta.$$

7.1. Time-domain recovery

The formulae presented so far is best suited for theoretical models that describe and solve the thermal response of geothermal heat exchangers in the complex-valued Laplace plane. To obtain the corresponding time evolution, the inverse Laplace transform is applied numerically to their outcomes [67].

Models that obtain the thermal response directly in the time domain do also exist. For them it is necessary to first obtain the inverse Laplace transform of Eq. (28) so that the outcome is incorporated into them. Fortunately, this can be accomplished analytically by combining three properties of the Laplace transform theory, namely, a shift in s of magnitude $\mathrm{Pe}^2/4$, the Laplace transform

$$\mathcal{L}\left[\left(\frac{\rho}{2}\right)^{|n|}\frac{e^{-\frac{\rho^2}{4\tau}}}{2\tau^{|n|+1}}\right]=\left(\sqrt{s}\right)^{|n|}K_n\left(\rho\sqrt{s}\right),$$

and the convolution theorem [60]. The result is the thermal influence exerted by a geothermal borehole onto its surrounding ground expressed directly in the time domain:

$$\Theta_{\mathrm{out}}=\mathrm{e}^{\frac{\rho\mathrm{Pe}}{2}\cos(\theta)}\int_0^{\tau}\frac{\mathrm{f}(\lambda)}{4\pi}\,\frac{\mathrm{e}^{-\frac{\rho^2}{4(\tau-\lambda)}-\frac{\mathrm{Pe}^2}{4}(\tau-\lambda)}}{(\tau-\lambda)}\,\mathrm{d}\lambda$$
$$+\ \mathrm{e}^{\frac{\rho\mathrm{Pe}}{2}\cos(\theta)}\rho\mathrm{e}^{+\imath\theta}\int_0^{\tau}A_{0(+1)}(\lambda)\,\frac{\mathrm{e}^{-\frac{\rho^2}{4(\tau-\lambda)}-\frac{\mathrm{Pe}^2}{4}(\tau-\lambda)}}{4\,(\tau-\lambda)^2}\,\mathrm{d}\lambda$$
$$+\ \mathrm{e}^{\frac{\rho\mathrm{Pe}}{2}\cos(\theta)}\rho\mathrm{e}^{-\imath\theta}\int_0^{\tau}A_{0(-1)}(\lambda)\,\frac{\mathrm{e}^{-\frac{\rho^2}{4(\tau-\lambda)}-\frac{\mathrm{Pe}^2}{4}(\tau-\lambda)}}{4\,(\tau-\lambda)^2}\,\mathrm{d}\lambda, \tag{29}$$

where

$$\mathrm{f}(\tau)=\sum_{j=1}^{N_p}\big[1-\mathrm{Pe}\,\pi\big(A_{0(+1)j}+A_{0(-1)j}\big)\big]\mathrm{q}_j(\tau)$$

and

$$A_{0(\pm1)}(\tau)=\sum_{j=1}^{N_p}A_{0(\pm1)j}\,\frac{\mathrm{q}_j(\tau)}{2\pi\kappa}.$$

The first term in Eq. (29) is well known from the state of art [19]. It represents the thermal influence exerted by a moving infinite line source of heat. The novelty of the present work resides in its mathematically rigorous derivation, using matched asymptotic expansion techniques, and in the presence of a fictitious heat injection rate per unit borehole length $\mathrm{f}(\tau)$ replacing the real one $\mathrm{q}(\tau)$.

Completely nonexistent in the prevailing literature are the second and third terms in Eq. (29). They represent higher order corrections that can only be envisioned and derived through mathematically rigorous approaches. These novel terms account for the spatial position of the pipes inside the borehole and their relevance seems *a-priori* high, based on the absence of a multiplying Peclet number in Eq. (29). But it was shown in Section 4 that this is not the case, with these terms indeed representing small corrections to the thermal influence of a borehole.

7.2. Constant heat injection rates

When heat injection rates per unit pipe length $\mathrm{q}_j(\tau)$ are constant in time, f and $A_{0(\pm1)}$ are constants as well. Then, Eq. (29) can be written in a more compact and enlightening way now that f and $A_{0(\pm1)}$ can be taken out of their respective integrals:

$$\Theta_{\mathrm{out}}=\frac{\mathrm{f}}{2\pi}\,\mathrm{e}^{\frac{\rho\mathrm{Pe}}{2}\cos(\theta)}\underline{K}_0\left(\frac{\rho\,\mathrm{Pe}}{2},\frac{\mathrm{Pe}^2}{4}\tau\right)$$
$$+\ A_{0(+1)}\mathrm{e}^{+\imath\theta}\frac{\mathrm{Pe}}{2}\,\mathrm{e}^{\frac{\rho\mathrm{Pe}}{2}\cos(\theta)}\underline{K}_1\left(\frac{\rho\,\mathrm{Pe}}{2},\frac{\mathrm{Pe}^2}{4}\tau\right)$$
$$+\ A_{0(-1)}\mathrm{e}^{-\imath\theta}\frac{\mathrm{Pe}}{2}\,\mathrm{e}^{\frac{\rho\mathrm{Pe}}{2}\cos(\theta)}\underline{K}_1\left(\frac{\rho\,\mathrm{Pe}}{2},\frac{\mathrm{Pe}^2}{4}\tau\right). \tag{30}$$

The functions $\underline{K}_n(z,w)$, defined as

$$\underline{K}_n(z,w)=\frac{1}{2}\left(\frac{z}{2}\right)^n\int_0^{w}\frac{e^{-\frac{z^2}{4\lambda}-\lambda}}{\lambda^{n+1}}\,\mathrm{d}\lambda,$$

hide now all the mathematical complexity of Eq. (30). Their nomenclature is chosen on purpose as they are closely related to the modified Bessel functions of the second kind $K_n(z)$ to which they converge when their second argument tends to infinity [62]:

$$\lim_{w\to\infty}\underline{K}_n(z,w)=K_n(z).$$

However, they should not be called incomplete modified Bessel functions of the second kind as better candidates for that name already exist in the literature [71].

Regarding the computation of $\underline{K}_n(z,w)$, these functions can handily be expressed in terms of generalized incomplete gamma functions whose evaluation has thoroughly been studied in the literature, both analytically [72–75] and numerically [76,77]. Since the present application leads to very demanding values for the arguments of $\underline{K}_n(z,w)$, the authors have developed their own expansions for the generalized incomplete gamma functions which outperform the existing ones [78].

Fig. 10 shows, for the borehole configuration considered in Section 4, the time evolution of the ground temperature on a circle located at a distance $\rho=5$ from the borehole. Left and right plots represent the evolution for two different values of the Peclet number, namely, 0.01 and 0.1 respectively, obtained from implementing in Fortran95 Eq. (30) and the expansions for $\underline{K}_n(z,x)$ [78].

First and foremost, the complete asymptotic solution as well as the zeroth order solution perform very good, with deviations from the reference solution that are negligible from an engineering point of view. The shown results also evidence the little impact the Peclet number of the groundwater flow has on the accuracy of the model, a conclusion in line with the observations made in Section 4.

The Peclet number of the groundwater flow has, however, a strong impact on the thermal influence of the borehole, as seen in Fig. 10. On one hand, the intensity of the thermal influence grows with decreasing Peclet numbers. This is a consequence of the inherent inefficiency of heat conduction that leads to a build up of heat around the borehole. This build up takes place in all spatial directions, not only downwards of the borehole, leading to the shift in temperatures observed on the left plot. On the other hand, the final steady-state of the thermal influence is reached sooner for increasing Peclet numbers of the groundwater

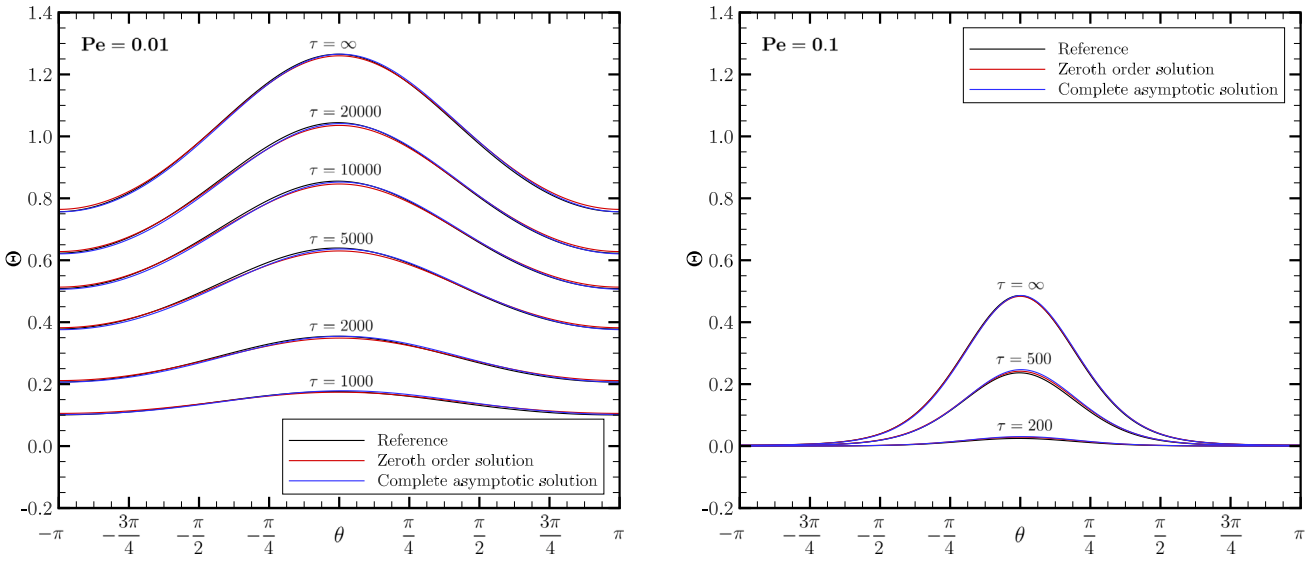

Fig. 10. Unsteady thermal influence of the borehole.

flow. This makes sense as the convective transport of heat is then more intense, washing away faster the intermediate temperature states.

The previous two statements regarding the influence of the Peclet number can also be inferred from Eq. (30). The aforementioned build up in temperatures is the result of ρPe becoming smaller in the argument of the exponential function. And the product $\mathrm{Pe}^2\tau$ becoming larger in the second argument of the functions $\underline{K}_n(z,w)$ is the reason for the faster transition towards the final steady-state.

7.3. Steady-state solution

The final steady state reached by the thermal influence of a geothermal borehole, with constant heat injection rates per unit pipe length, can be obtained in two different ways. The first one consists in letting τ tend to infinity in Eq. (30). This approach exploits that $\underline{K}_n(z,w)$ tends to the modified Bessel function of the second kind $K_n(z)$ under that limit. The second one consists in using the Final Value Theorem applied to Eq. (28) [60]. Both approaches obviously lead to the same result:

$$\begin{aligned}\Theta_{\mathrm{out}}\big|_{\tau\to\infty} &= \frac{\mathrm{f}}{2\pi}\,\mathrm{e}^{\frac{\rho\mathrm{Pe}}{2}\cos(\theta)}K_0\left(\frac{\rho\,\mathrm{Pe}}{2}\right)\\ &+ A_{0(+1)}\mathrm{e}^{+\imath\theta}\frac{\mathrm{Pe}}{2}\,\mathrm{e}^{\frac{\rho\mathrm{Pe}}{2}\cos(\theta)}K_1\left(\frac{\rho\,\mathrm{Pe}}{2}\right)\\ &+ A_{0(-1)}\mathrm{e}^{-\imath\theta}\frac{\mathrm{Pe}}{2}\,\mathrm{e}^{\frac{\rho\mathrm{Pe}}{2}\cos(\theta)}K_1\left(\frac{\rho\,\mathrm{Pe}}{2}\right).\end{aligned}$$

Fig. 11 shows, for the borehole configuration considered in Section 4, the steady-state ground temperature on a circle located at the distance $\rho = 50$ from the borehole center. The plotted results, obtained from implementing in Fortran95 the previous equation, evidence once again the capability of the proposed model to correctly predict the thermal influence of a borehole, regardless of the Peclet number of the groundwater flow. Also the build up of heat around the borehole, pointed out in the previous section, and its dependence on the Peclet number are perfectly identifiable in Fig. 11 in which results for Peclet numbers up to 10 are represented.

7.4. Purely-conducting limit

Whenever an existing model is improved by the addition of a new physical phenomenon, it is desirable that the resulting model reverts to the existing one whenever the new phenomenon becomes negligible. For the present work it means the developed formulae should revert to the purely-conducting case for vanishing groundwater velocities.

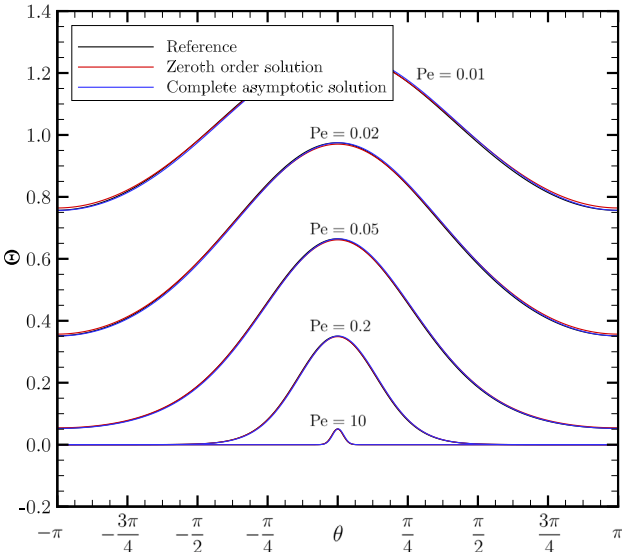

Fig. 11. Steady-state thermal influence of the borehole.

The purely-conducting limit of the thermal influence exerted by a borehole onto its surrounding ground is obtained by letting the Peclet number tend to zero in any of the expressions presented in Section 7. The best suited expression for that is Eq. (29) which simplifies to

$$\begin{aligned}\Theta_{\mathrm{out}} &= \int_0^\tau \frac{\mathrm{f}(\lambda)}{4\pi}\,\frac{\mathrm{e}^{-\frac{\rho^2}{4(\tau-\lambda)}}}{(\tau-\lambda)}\,\mathrm{d}\lambda\\ &+ \rho\mathrm{e}^{+\imath\theta}\int_0^\tau A_{0(+1)}(\lambda)\,\frac{\mathrm{e}^{-\frac{\rho^2}{4(\tau-\lambda)}}}{4\,(\tau-\lambda)^2}\,\mathrm{d}\lambda\\ &+ \rho\mathrm{e}^{-\imath\theta}\int_0^\tau A_{0(-1)}(\lambda)\,\frac{\mathrm{e}^{-\frac{\rho^2}{4(\tau-\lambda)}}}{4\,(\tau-\lambda)^2}\,\mathrm{d}\lambda\end{aligned}\tag{31}$$

with

$$\mathrm{f}(\tau) = \sum_{j=1}^{N_p}\mathrm{q}_j(\tau) = \mathrm{q}(\tau).$$

The first term in Eq. (31) is again well known from the state of the art [19]. It represents the thermal influence exerted by an infinite line

source of heat. Again, the novelty of the present work resides in the followed derivation procedure and not in the term itself. The remaining two terms are again the higher order corrections introduced here for the first time.

Finally, and for the sake of completeness, for constant heat injection rates per unit pipe length a simpler and more convenient expression for the thermal influence of a borehole is obtained, namely,

$$\Theta_{\text{out}} = \frac{\mathfrak{q}}{4\pi} E_1\left(\frac{\rho^2}{4\tau}\right) + \left(A_{0(+1)}\mathrm{e}^{+\imath\theta} + A_{0(-1)}\mathrm{e}^{-\imath\theta}\right)\frac{\mathrm{e}^{-\frac{\rho^2}{4\tau}}}{\rho},$$

in which $E_1(z)$ represents the exponential integral [62]. As well known for two-dimensional heat conduction problems, no steady state solution exists in this case [19].

8. Conclusions

The performance of geothermal heat exchangers relies heavily on the thermal characteristics of the ground, being the slowness of heat conduction the main limiting factor. When aquifers are present, though, the thermal capabilities of the ground improve a lot, enabling the construction of more compact and affordable heat exchangers. Of course, theoretical models for the interaction of geothermal boreholes with groundwater flows are required for the design of such geothermal heat exchangers.

The present work has developed one such model for the case of creeping groundwater flows. In them, the convective transport of heat is weak enough that the Peclet number of the flow is small compared to unity. Additionally, heating and cooling needs of the building are assumed to vary slowly, a simplification that matches most operating conditions of real-world geothermal HVAC systems.

Scale analysis of the considered heat transfer problem has revealed the existence of two distinct regions. The inner region encompasses the borehole and the ground located close to the borehole. In it, heat conduction dominates, with heat convection and thermal inertia being second and third ranked, respectively. The relevance of the different phenomena changes, though, further away from the borehole giving rise to the outer region. In the distinguished limit considered in the present work, all three physical phenomena are equally important in the outer region.

The developed model for the interaction of geothermal boreholes with groundwater flows is the result of exploiting the aforementioned two-region structure using matched asymptotic expansion techniques. For the solution to the outer region, closed-form expressions have been obtained. For the solution to the inner region, though, only semi-analytical results have been presented, with the derivation of closed-form expressions postponed to a follow-up work by the authors.

Comparisons with detailed numerical simulations of the complete heat transfer problem have shown that the proposed model exceeds by an order of magnitude the accuracy of the state of the art, leading to absolute (relative) errors below 0.03 (2.3%). This is accomplished by incorporating, for the first time, azimuthal corrections which can only be envisioned and derived following rigorous mathematical approaches, something the state of the art was lacking. The performed comparisons have also highlighted the limitations of the proposed model as its accuracy worsens when the assumptions underlying the performed asymptotic analysis are not met. That is, when the Peclet number becomes of order unity or the heating and cooling needs change too fast.

The proposed model has also served to assess, for the first time, the theoretical and conceptual merits and limits of the state of the art. Thanks to its underlying asymptotic analysis it is now proven that ideas, concepts, and modeling approaches meant for purely-conducting grounds are also applicable to grounds with creeping groundwater flows. It has also been shown that the state of the art coincides with the zeroth order solution derived in the present work and that some of the improvements proposed in the literature, like the infinite cylindrical source models, have in reality a limited impact onto the accuracy of the results.

The next step in the roadmap of the authors is the development of a model valid for stronger groundwater flows with Peclet numbers of order unity. The interest in such a model is threefold. First, geothermal piles, with their larger borehole radii, lead to larger Peclet numbers for the groundwater flow. Second, analysis of geothermal boreholes in fracturated igneous and metamorphic grounds becomes feasible. And third, it represents the next logical step in the development of a single theoretical model valid for all Peclet numbers.

Declaration of competing interest

The authors declare that they have no known competing financial interests or personal relationships that could have appeared to influence the work reported in this paper.

Data availability

Data will be made available on request.

Acknowledgments

Grant PID2021-128172OB-I00 funded by MCIN/AEI/10.13039/501100011033, Spain and by “ERDF A way of making Europe”.

References

[1] International Energy Agency, Renewables 2021: Analysis and forecast to 2026, 2021, Paris, France.
[2] S. Chen, J. Mao, X. Han, Heat transfer analysis of a vertical ground heat exchanger using numerical simulation and multiple regression model, Energy Build. 129 (2016) 81–91, http://dx.doi.org/10.1016/j.enbuild.2016.07.010.
[3] A.D. Chiasson, S.J. Rees, J.D. Spitler, A preliminary assessment of the effects of groundwater flow on closed-loop ground-source heat pump systems, ASHRAE Trans 106 (1) (2000) 380–393.
[4] P. Conti, D. Testi, W. Grassi, Transient forced convection from an infinite cylindrical heat source in a saturated Darcian porous medium, Int. J. Heat Mass Transfer 117 (2018) 154–166, http://dx.doi.org/10.1016/j.ijheatmasstransfer.2017.10.012.
[5] R. Fan, Y. Jiang, Y. Yao, D. Shiming, Z. Ma, A study on the performance of a geothermal heat exchanger under coupled heat conduction and groundwater advection, Energy 32 (2017) 2199–2209, http://dx.doi.org/10.1016/j.energy.2007.05.001.
[6] J. Hecht-Méndez, N. Molina-Giraldo, P. Blum, P. Bayer, Evaluating MT3DMS for heat transport simulation of closed geothermal systems, Ground Water 48 (5) (2010) 741–756, http://dx.doi.org/10.1111/j.1745-6584.2010.00678.x.
[7] B. Li, Z. Han, X. Meng, H. Zhang, Study on the influence of the design method of the ground source heat pump system with considering groundwater seepage, Appl. Therm. Eng. 160 (2019) 114016, http://dx.doi.org/10.1016/j.applthermaleng.2019.114016.
[8] Y. Lou, P. fei Fang, X. yu Xie, C.S.A. Chong, F. yuan Li, C. yang Liu, Z. jin Wang, D. yong Zhu, Numerical research on thermal response for geothermal energy pile groups under groundwater flow, Geomech. Energy Environ. 28 (2021) 100257, http://dx.doi.org/10.1016/j.gete.2021.100257.
[9] Y. Nam, R. Ooka, S. Hwang, Development of a numerical model to predict heat exchange rates for a ground-source heat pump system, Energy Build. 40 (12) (2008) 2133–2140, http://dx.doi.org/10.1016/j.enbuild.2008.06.004.
[10] Y. Niibori, Y. Iwata, S. Ichinose, G. Fukaya, Design of the BHP system considering the heat transport of groundwater flow, in: Proceedings of the World Geothermal Congress 2005, Antalya, Turkey, 2005.
[11] J. Raymond, R. Therrien, L. Gosselin, R. Lefebvre, Numerical analysis of thermal response tests with a groundwater flow and heat transfer model, Renew. Energy 36 (1) (2011) 315–324, http://dx.doi.org/10.1016/j.renene.2010.06.044.
[12] P. Cui, W. Yang, W. Zhang, K. Zhu, J.D. Spitler, M. Yu, Advances in ground heat exchangers for space heating and cooling: Review and perspectives, Energy Built Environ (2023) In press, http://dx.doi.org/10.1016/j.enbenv.2022.10.002.
[13] M. Li, A.C.K. Lai, Review of analytical models for heat transfer by vertical ground heat exchangers (GHEs): A perspective of time and space scales, Appl. Energy 151 (2015) 178–191, http://dx.doi.org/10.1016/j.apenergy.2015.04.070.
[14] A. Capozza, M.D. Carli, A. Zarrella, Investigations on the influence of aquifers on the ground temperature in ground-source heat pump operation, Appl. Energy 107 (2013) 350–363, http://dx.doi.org/10.1016/j.apenergy.2013.02.043.

[15] G. Jia, Z. Ma, Z. Xia, J. Wang, Y. Zhang, L. Jin, Influence of groundwater flow on the ground heat exchanger performance and ground temperature distributions: A comprehensive review of analytical, numerical and experimental studies, Geothermics 100 (2022) 102342, http://dx.doi.org/10.1016/j.geothermics.2021.102342.
[16] J. Rico, M. Hermanns, Modeling the thermal interaction of geothermal boreholes with aquifers using asymptotic expansion techniques, IOP Conf Ser: Earth Environ Sci 588 (5) (2020) 052033, http://dx.doi.org/10.1088/1755-1315/588/5/052033.
[17] A. Chiasson, A. O'Connell, New analytical solution for sizing vertical borehole ground heat exchangers in environments with significant groundwater flow: Parameter estimation from thermal response test data, HVAC&R Res 17 (6) (2011) 1000–1011, http://dx.doi.org/10.1080/10789669.2011.609926.
[18] Z. Zhao, Y.-F. Lin, A. Stumpf, X. Wang, Assessing impacts of groundwater on geothermal heat exchangers: A review of methodology and modeling, Renew. Energy 190 (2022) 121–147, http://dx.doi.org/10.1016/j.renene.2022.03.089.
[19] H. Carslaw, J. Jaeger, Conduction of Heat in Solids, second ed., Oxford University Press, Oxford, 1959.
[20] N. Diao, Q. Li, Z. Fang, Heat transfer in ground heat exchangers with groundwater advection, Int. J. Therm. Sci. 43 (12) (2004) 1203–1211.
[21] J. Hecht-Méndez, M. de Paly, M. Beck, P. Bayer, Optimization of energy extraction for vertical closed-loop geothermal systems considering groundwater flow, Energy Convers. Manage. 66 (2013) 1–10, http://dx.doi.org/10.1016/j.enconman.2012.09.019.
[22] T. Metzger, S. Didierjean, D. Maillet, Optimal experimental estimation of thermal dispersion coefficients in porous media, Int. J. Heat Mass Transfer 47 (2004) 3341–3353, http://dx.doi.org/10.1016/j.ijheatmasstransfer.2004.02.024.
[23] M.G. Sutton, D.W. Nutter, R.J. Couvillion, A ground resistance for vertical bore heat exchangers with groundwater flow, J. Energy Resour. Technol. 125 (3) (2003) 183–189, http://dx.doi.org/10.1115/1.1591203.
[24] M. Verdoya, P. Chiozzi, Influence of groundwater flow on the estimation of subsurface thermal parameters, Int. J. Earth Sci. 107 (2018) 137–144, http://dx.doi.org/10.1007/s00531-016-1397-x.
[25] M. Verdoya, C. Pacetti, P. Chiozzi, C. Invernizzi, Thermophysical parameters from laboratory measurements and in-situ tests in borehole heat exchangers, Appl. Therm. Eng. 144 (2018) 711–720, http://dx.doi.org/10.1016/j.applthermaleng.2018.08.039.
[26] J. Claesson, G. Hellström, Analytical studies of the influence of regional groundwater flow by on the performance of borehole heat exchangers, in: 8th International Conference on Thermal Energy Storage, 2000.
[27] S. Erol, B. François, Multilayer analytical model for vertical ground heat exchanger with groundwater flow, Geothermics 71 (2018) 294–305, http://dx.doi.org/10.1016/j.geothermics.2017.09.008.
[28] S. Erol, M.A. Hashemi, B. François, Analytical solution of discontinuous heat extraction for sustainability and recovery aspects of borehole heat exchangers, Int. J. Therm. Sci. 88 (2015) 47–58, http://dx.doi.org/10.1016/j.ijthermalsci.2014.09.007.
[29] P. Eskilson, Thermal Analysis of Heat Extraction Boreholes (Ph.D. thesis), Department of Mathematical Physics, Lund Institute of Technology, Lund, Sweden, 1987.
[30] Y. Guo, X. Hu, J. Banks, W. Liu, Considering buried depth in the moving finite line source model for vertical borehole heat exchangers — A new solution, Energy Build. 214 (2020) 109859, http://dx.doi.org/10.1016/j.enbuild.2020.109859.
[31] J. Hu, An improved analytical model for vertical borehole ground heat exchanger with multiple-layer substrates and groundwater flow, Appl. Energy 202 (2017) 537–549, http://dx.doi.org/10.1016/j.apenergy.2017.05.152.
[32] N. Molina-Giraldo, P. Blum, K. Zhu, P. Bayer, Z. Fang, A moving finite line source model to simulate borehole heat exchangers with groundwater advection, Int. J. Therm. Sci. 50 (12) (2011) 2506–2513, http://dx.doi.org/10.1016/j.ijthermalsci.2011.06.012.
[33] J.A. Rivera, P. Blum, P. Bayer, Ground energy balance for borehole heat exchangers: Vertical fluxes, groundwater and storage, Renew. Energy 83 (2015) 1341–1351, http://dx.doi.org/10.1016/j.renene.2015.05.051.
[34] J.A. Rivera, P. Blum, P. Bayer, A finite line source model with Cauchy-type top boundary conditions for simulating near surface effects on borehole heat exchangers, Energy 98 (2016) 50–63, http://dx.doi.org/10.1016/j.energy.2015.12.129.
[35] J.A. Rivera, P. Blum, P. Bayer, Influence of spatially variable ground heat flux on closed-loop geothermal systems: Line source model with nonhomogeneous Cauchy-type top boundary conditions, Appl. Energy 180 (2016) 572–585, http://dx.doi.org/10.1016/j.apenergy.2016.06.074.
[36] Z. Wenke, Z. Linhua, G. Yan, G. Xiang, Z. Hao, Y. Mingzhi, The annual fluctuation of underground temperature response caused by ground heat exchanger in the condition of groundwater seepage, Energy Build. 186 (2019) 37–45, http://dx.doi.org/10.1016/j.enbuild.2019.01.004.
[37] R. Al-Khoury, N. BniLam, M.M. Arzanfudi, S. Saeid, A spectral model for a moving cylindrical heat source in a conductive-convective domain, Int. J. Heat Mass Transfer 163 (2020) 120517, http://dx.doi.org/10.1016/j.ijheatmasstransfer.2020.120517.
[38] R. Al-Khoury, N. BniLam, M.M. Arzanfudi, S. Saeid, Analytical model for arbitrarily configured neighboring shallow geothermal installations in the presence of groundwater flow, Geothermics 93 (2021) 102063, http://dx.doi.org/10.1016/j.geothermics.2021.102063.
[39] T. Katsura, Y. Shoji, Y. Sakata, K. Nagano, Erratum to "Method for calculation of ground temperature in scenarios involving multiple ground heat exchangers and groundwater advection" [Energy Build. 220 (2020) 110000], Energy Build. 227 (2020) 110409, http://dx.doi.org/10.1016/j.enbuild.2020.110409.
[40] T. Katsura, Y. Shoji, Y. Sakata, K. Nagano, Method for calculation of ground temperature in scenario involving multiple ground heat exchangers considering groundwater advection, Energy Build. 220 (2020) 110000, http://dx.doi.org/10.1016/j.enbuild.2020.110000.
[41] S. Cai, X. Li, M. Zhang, J. Fallon, K. Li, T. Cui, An analytical full-scale model to predict thermal response in boreholes with groundwater advection, Appl. Therm. Eng. 168 (2020) 114828, http://dx.doi.org/10.1016/j.applthermaleng.2019.114828.
[42] S. Düber, M. Ziegler, R. Fuentes, Development and validation of a computationally efficient hybrid model for temporal high-resolution simulations of geothermal bore fields, Int. J. Numer. Anal. Methods Geomech. 46 (14) (2022) 2792–2813, http://dx.doi.org/10.1002/nag.3427.
[43] M. Tye-Gingras, L. Gosselin, Generic ground response functions for ground exchangers in the presence of groundwater flow, Renew. Energy 72 (2014) 354–366, http://dx.doi.org/10.1016/j.renene.2014.07.026.
[44] C. Wang, X. Wang, J. Lu, Y. Lu, Y. Sun, P. Zhang, A semi-analytical heat transfer model for deep borehole heat exchanger considering groundwater seepage, Int. J. Therm. Sci. 175 (2022) 107465, http://dx.doi.org/10.1016/j.ijthermalsci.2022.107465.
[45] M. Hermanns, New generation of theoretical models for the thermal response of geothermal heat exchangers, IOP Conf. Ser.: Earth Environ. Sci. 410 (2020) 012042, http://dx.doi.org/10.1088/1755-1315/410/1/012042.
[46] M. Hermanns, Modelling the thermal response of geothermal heat exchangers using asymptotic expansion techniques, in: Proceedings of the World Geothermal Congress 2020+1, Reykjavik, Iceland, 2021.
[47] M. Hermanns, J.M. Pérez, Asymptotic analysis of vertical geothermal boreholes in the limit of slowly varying heat injection rates, SIAM J. Appl. Math. 74 (1) (2014) 60–82, http://dx.doi.org/10.1137/130930170.
[48] M. Hermanns, S. Ibáñez, Thermal response of slender geothermal boreholes to subannual harmonic excitations, SIAM J. Appl. Math. 79 (1) (2019) 230–256, http://dx.doi.org/10.1137/17M1161324.
[49] M. Hermanns, S. Ibáñez, Harmonic thermal response of thermally interacting geothermal boreholes, SIAM J. Appl. Math. 80 (1) (2020) 262–288, http://dx.doi.org/10.1137/18M119001X.
[50] M. Hermanns, J.M. Rivero, On the symmetry properties of the network of thermal resistances representing the thermal response of slender geothermal boreholes, Geothermics 94 (2021) 102078, http://dx.doi.org/10.1016/j.geothermics.2021.102078.
[51] M. Hermanns, J.M. Rivero, On the quasi-steady limit of the enhanced multipole method for the thermal response of geothermal boreholes, Appl. Therm. Eng. 225 (2023) 120121, http://dx.doi.org/10.1016/j.applthermaleng.2023.120121.
[52] S. Ibáñez, M. Hermanns, On the steady-state thermal response of slender geothermal boreholes, SIAM J. Appl. Math. 78 (3) (2018) 1658–1681, http://dx.doi.org/10.1137/17M1122566.
[53] J.M. Rivero, M. Hermanns, Enhanced multipole method for the transient thermal response of slender geothermal boreholes, Int. J. Therm. Sci. 164 (2021) 106531, http://dx.doi.org/10.1016/j.ijthermalsci.2020.106531.
[54] A. Bejan, Convection Heat Transfer, third ed., Wiley, Hoboken, NJ, 2004.
[55] D.A. Nield, A. Bejan, Convection in Porous Media, fifth ed., Springer, Cham, 2017.
[56] G.K. Batchelor, An Introduction to Fluid Dynamics, second ed., Cambridge University Press, Cambridge, 2000.
[57] J. Bennet, J. Claesson, G. Hellström, Multipole Method to Compute the Conductive Heat Flows to and Between Pipes in a Composite Cylinder, Tech. Rep., Department of Building Technology and Mathematical Physics, Lund Institute of Technology, Lund, Sweden, 1987.
[58] J. Claesson, J. Bennet, Multipole method to compute the conductive heat flows to and between pipes in a cylinder, Department of Building Technology and Mathematical Physics, Lund Institute of Technology, Lund, Sweden, 1987.
[59] J. Claesson, G. Hellström, Multipole method to calculate borehole thermal resistances in a borehole heat exchanger, HVAC&R Research 17 (6) (2011) 895–911, http://dx.doi.org/10.1080/10789669.2011.609927.
[60] W.E. Boyce, R.C. DiPrima, D.B. Meade, Elementary Differential Equations and Boundary Value Problems, eleventh ed., Wiley, Hoboken, NJ, 2017.
[61] P.A. Lagerstrom, Matched Asymptotic Expansions: Ideas and Techniques, Springer, New York, 1988.
[62] F.W. Olver, D.W. Lozier, R.F. Boisvert, C.W. Clark (Eds.), NIST Handbook of Mathematical Functions, Cambridge University Press, New York, 2010.
[63] C. Inc., COMSOL multiphysics version 5.4. Reference manual, 2018, https://www.comsol.com/.
[64] S. Zhang, J. Jin, Computation of Special Functions, John Wiley & Sons Inc., New York, 1996.
[65] B. Badenes, B. Sanner, M.Á. Mateo Pla, J.M. Cuevas, F. Bartoli, F. Ciardelli, R.M. González, A.N. Ghafar, P. Fontana, L.L. Zuñiga, J.F. Urchueguía, Development of

advanced materials guided by numerical simulations to improve performance and cost-efficiency of borehole heat exchangers (BHEs), Energy 201 (2020) 117628, http://dx.doi.org/10.1016/j.energy.2020.117628.

[66] V. Gnielinski, Turbulent heat transfer in annular spaces – A new comprehensive correlation, Heat Transf. Eng. 36 (9) (2015) 787–789, http://dx.doi.org/10.1080/01457632.2015.962953.

[67] M. Hermanns, Fast inverse Laplace transform for the unsteady thermal response of geothermal heat exchangers, AIP Conf. Proc. 2186 (1) (2019) 170002, http://dx.doi.org/10.1063/1.5138081.

[68] L.R. Ingersoll, O.J. Zabel, A.C. Ingersoll, Heat Conduction - With Engineering, Geological, and other Applications, University of Wisconsin Press, Madison, WI, 1954.

[69] L. Lamarche, S. Kajl, B. Beauchamp, A review of methods to evaluate borehole thermal resistances in geothermal heat-pump systems, Geothermics 39 (2) (2010) 187–200, http://dx.doi.org/10.1016/j.geothermics.2010.03.003.

[70] J. Rico, M. Hermanns, On the network of thermal resistances embodying the response of geothermal boreholes to creeping groundwater flows, Int. J. Thermal Sci. (2023) (In preparation).

[71] F.E. Harris, Incomplete bessel, generalized incomplete gamma, or leaky aquifer functions, J. Comput. Appl. Math. 215 (1) (2008) 260–269, http://dx.doi.org/10.1016/j.cam.2007.04.008.

[72] M. Boudjelkha, M.A. Chaudhry, On the approximation of a generalized incomplete gamma function arising in heat conduction problems, J. Math. Anal. Appl. 248 (2) (2000) 509–519, http://dx.doi.org/10.1006/jmaa.2000.6925.

[73] M.A. Chaudhry, N. Temme, E. Veling, Asymptotics and closed form of a generalized incomplete gamma function, J. Comput. Appl. Math. 67 (2) (1996) 371–379, http://dx.doi.org/10.1016/0377-0427(95)00018-6.

[74] M.A. Chaudhry, S.M. Zubair, Generalized incomplete gamma functions with applications, J. Comput. Appl. Math. 55 (1) (1994) 99–123, http://dx.doi.org/10.1016/0377-0427(94)90187-2.

[75] M.A. Chaudhry, S.M. Zubair, On a Class of Incomplete Gamma Functions with Applications, Chapman and Hall/CRC, New York, 2001.

[76] N.M. Temme, The leaky aquifer function revisited, Int. J. Quantum Chem. 109 (13) (2009) 2826–2830, http://dx.doi.org/10.1002/qua.22130.

[77] V. Numerics, IMSL MATH/LIBRARY FORTRAN subroutines for mathematical applications, 1991, Houston.

[78] J. Rico, M. Hermanns, Computation of generalized incomplete gamma functions for parameter values spanning several orders of magnitude, J. Comput. Appl. Math. (2023) (in preparation).